



저작자표시-비영리-변경금지 2.0 대한민국

이용자는 아래의 조건을 따르는 경우에 한하여 자유롭게

- 이 저작물을 복제, 배포, 전송, 전시, 공연 및 방송할 수 있습니다.

다음과 같은 조건을 따라야 합니다:



저작자표시. 귀하는 원저작자를 표시하여야 합니다.



비영리. 귀하는 이 저작물을 영리 목적으로 이용할 수 없습니다.



변경금지. 귀하는 이 저작물을 개작, 변형 또는 가공할 수 없습니다.

- 귀하는, 이 저작물의 재이용이나 배포의 경우, 이 저작물에 적용된 이용허락조건을 명확하게 나타내어야 합니다.
- 저작권자로부터 별도의 허가를 받으면 이러한 조건들은 적용되지 않습니다.

저작권법에 따른 이용자의 권리는 위의 내용에 의하여 영향을 받지 않습니다.

이것은 [이용허락규약\(Legal Code\)](#)을 이해하기 쉽게 요약한 것입니다.

[Disclaimer](#)

Master's Thesis of Engineering

**A Study on the Repair Method
of Roof Members
in Wooden-Structural Heritage**

전통 목조 건축물의 지붕 부재
보수보강에 관한 연구

August 2021

**Graduate School of Engineering
Seoul National University
Architecture and Architectural Engineering**

Seo Hyung Lee

A Study on the Repair Method of Roof Members in Wooden-Structural Heritage

Advisor: Sung Gul Hong

**Submitting a Master's thesis of
Architecture and Architectural Engineering**

August 2021

**Graduate School of Engineering
Seoul National University
Architecture and Architectural Engineering**

Seo Hyung Lee

**Confirming the Master's thesis written by
Seo Hyung Lee**

July 2021

Chair	Hong Gun Park
Vice Chair	Sung Gul Hong
Examiner	Cheol Ho Lee

Abstract

A Study on the Repair Method of Roof Members in Wooden-Structural Heritage

Lee, Seo hyung

Department of Architecture and Architectural Engineering

College of Engineering

Seoul National University

Traditional wooden structures occupy a large proportion of national cultural structures. Over time, traditional wooden structures are subject to damage from various factors. In accordance with the Cultural Heritage Protection Act, the old traditional wooden structures are being continuously repaired. During repair work, the repair standards for damaged members are not clear, so it is common to replace them with new materials, and excessive replacement is being made. In this study, to prevent reckless replacement of reusable old members, the study was conducted on the repair and reinforcement of roof members of traditional wooden structures.

Currently, study related to traditional wooden structures mainly focuses on the stiffness of wooden joints, and there is a lack of study on repair and

Abstract

reinforcement of member. Therefore, in this study, the roof members of Jeongyodang Hall in Dosanseowon Confucian School, Lecture Hall of Sosu Confucian Academy, Yangjindang House, Namhansanseong Suengyeoljeon Hall were provided by the foundation, and structural analysis, non-destructive diagnostic test, repair design, and cross-sectional analysis were conducted using these materials.

The structural vulnerable part of the member was reviewed through the structural analysis of the member of the wooden structures, and the naturally occurring decay vulnerability was investigated through a non-destructive diagnostic test. In the repair design, the traditional carpentry method suitable for the load conditions of each member was applied through a case study. To verify the performance of the joint, a flexural test was performed that conforms to the load conditions for each member.

The flexural strength, flexural stiffness, and ductility were calculated as the results of the experiment. The flexural strength and initial stiffness showed a tendency to increase or decrease at a similar rate. The modified butt joint and the tusk tenon joint were analyzed through an equivalent sectional model. The equivalent sectional model showed good performance in predicting the initial stiffness.

Except for Chu-nyu, related studies on small roof members (Yeon-mok, Bu-yeon, Mok-gi-yeon, etc.) are lacking. Therefore, it is expected that the model proposed in this study can be used as basic research data.

Keywords : Traditional wooden structures, Roof member, Non-destructive diagnostic test, repair and reinforcement, section analysis model

Student Number : 2019-23472

Contents

Abstract	i
Contents	iv
List of Tables	vii
List of Figures	ix
Chapter 1. Introduction	1
1.1 Background.....	1
1.2 Scope and Objectives.....	3
Chapter 2. Literature Review	5
2.1 Code Review	5
2.1.1 KS, KDS	5
2.1.2 ISO.....	6
2.1.3 ICOMOS.....	6
2.2 Literature Review	8
2.2.1 Strutral analysis of traditional wooden building.....	8
2.2.2 Non-destructive diagnosic test.....	9
2.2.3 The structural strengthening characteristic of Chu-nyu.....	12
Chapter 3. Structural analysis	15
3.1 Introduction	15
3.2 Design allowable stress	16
3.3 Structural analysis by member	18

3.3.1 Chu-nyu	18
3.3.2 Yeon-mok.....	19
3.3.3 Bu-yeon	21
3.3.4 Mok-gi-yeon.....	22
3.4 Structural analysis results and discussion.....	24

Chapter 4. Non-destructive diagnostic test of damaged member..... 32

4.1 Non-destructive diagnostic test	32
4.1.1 Stress wave test.....	33
4.1.2 Drill resistance test	35
4.1.3 Non-destructive diagnostic test results (Refer to Appendix. A)	37
4.2 Residual strength experiment	41
4.3 Conclusion.....	44

Chapter 5. Repair design and experiments..... 46

5.1 Repair design and experiment.	46
5.1.1 Material property	46
5.1.2 Chu-nyu	48
5.1.3 Yeon-mok.....	52
5.1.4 Bu-yeon	54
5.1.5 Mok-gi-yeon.....	57
5.2 Experiment results and discussions	60
5.2.1 Load-displacement Curve.....	60
5.2.2 Strength.....	63
5.2.3 Stiffness	66
5.2.4 Ductility.....	70
5.2.5 Experimental value comparing theoretical value of reference	73
5.3 Section analysis model	75

Contents

5.3.1 Chu-nyu	75
5.3.2 Yeon-mok.....	75
5.3.3 Bu-yeon, Mok-gi-yeon	79
Chapter 6. Conclusion.....	83
Appendix. A. List of non-destructive test results	85
Appendix. B. Failure mode of flexural test	98
References	106
초 목	109

List of Tables

Table 2-1 KS, KDS related to wooden joint.....	5
Table 2-2 ISO related to wooden joint.....	6
Table 3-1 Standard allowable stress for visual grade structural members, which are conifers (KDS 41 33 02 Table 1.1-4).....	16
Table 3-2 modification factor of allowable design stress (KDS 41 33 02 Table.1.1-6).....	17
Table 3-3 Chu-nyu length and height measurement of each building..	19
Table 3-4 The soil thickness of each structure.....	20
Table 3-5 The horizontal length of each structure	21
Table 3-6 Measuring of horizontal length of Bu-yeon	22
Table 3-7 The horizontal length of each structure	23
Table 3-8 Structural analysis results of Jeongyodang Hall.....	26
Table 3-9 Structural analysis results of Lecture Hall of Sosu	27
Table 3-10 Structural analysis results of Yangjindang House	28
Table 3-11 Structural analysis results of Suengyeoljeon Hall	29
Table 3-12 Result of Allowable stress ratio.....	30
Table 3-13 vulnerable part of roof member	31
Table 4-1 Dismantling member experiment detail	40
Table 4-2 Bending test result of Yeon-mok	43
Table 5-1 Wood (KS F 2206,2208,2209).....	47
Table 5-2 Titanium bar	47
Table 5-3 The distance according to the diameter of the titanium shear connector	47
Table 5-4 Load and displacement (Chu-nyu)	63
Table 5-5 Load and displacement (Jang-yeon).....	63
Table 5-6 Load and displacement (Dan-yeon)	64

List of Tables

Table 5-7 Load and displacement (Bu-yeon)	64
Table 5-8 Load and displacement (Mok-gi-yeon)	65
Table 5-9 Stiffness (Chu-nyu)	67
Table 5-10 Stiffness (Jang-yeon)	67
Table 5-11 Stiffness (Dan-yeon).....	68
Table 5-12 Stiffness (Bu-yeon).....	68
Table 5-13 Stiffness (Mok-gi-yeon)	69
Table 5-14 Ductility (Chu-nyu)	70
Table 5-15 Ductility (Jang-yeon)	71
Table 5-16 Ductility (Dan-yeon)	71
Table 5-17 Ductility (Bu-yeon)	72
Table 5-18 Ductility (Mok-gi-yeon).....	72
Table 5-19 Experimental value comparing theoretical value of reference member	74
Table 5-20 Flexural strength and initial stiffness (Jang-yeon)	78
Table 5-21 Flexural strength and initial stiffness (Dan-yeon)	78
Table 5-22 Flexural strength and initial stiffness (Bu-yeon)	81
Table 5-23 Flexural strength and initial stiffness (Mok-gi-yeon).....	82

List of Figures

Figure 2-1 3D Modeling of Musangsujeon	8
Figure 2-2 Modeling the support condition.....	8
Figure 2-3 Allowable stress analysis result of roof member	9
Figure 2-4 The evaluated woods for NDT study	10
Figure 2-5 Measured positions of non-destructive testing in woods....	10
Figure 2-6 USW and ratio of decay length caused by DRT.	11
Figure 2-7 The comparison of artificial picture and real cross-section.	11
Figure 2-8 The slope of a roof and structural points of Chu-nyu	12
Figure 2-9 Elevation and section views of Chu-nyu	13
Figure 2-10 The experimental setup of Chu-nyu.....	13
Figure 2-11 Comparison of load-deflection curves of specimens	14
Figure 2-12 Comparison of ductility of specimens	14
Figure 3-1 Length and height measurement for structural review of Chu-nyu	18
Figure 3-2 Example of Yeon-mok in the form of a simple beam	19
Figure 3-3 Location of $h_1 \sim h_4$ for calculation of soil thickness.....	20
Figure 3-4 Model for measuring the horizontal length of Yeon-mok... 20	
Figure 3-5 Calculation of reaction point for structural review of Bu-yeon	22
Figure 3-6 Model for measuring the horizontal length of Mok-gi-yeon	23
Figure 4-1 Stress wave measuring device (Metriguard 239A).....	34
Figure 4-2 Stress wave test method.....	35
Figure 4-3 Drill resistance device (IML F500-S).....	36
Figure 4-4 Drill resistance test.....	36
Figure 4-5 Flexural test	41

List of Figures

Figure 5-1 Detail of the reference member (Chu-nyu).....	49
Figure 5-2 Detail of the repaired member (Chu-nyu).....	50
Figure 5-3 Titanium bar and inserting process	50
Figure 5-4 Test set-up (Chu-nyu)	51
Figure 5-5 The modified butt joint	52
Figure 5-6 Detail of the repaired member (Yeon-mok).....	53
Figure 5-7 Test set-up (Yeon-mok).....	54
Figure 5-8 The tusk tenon joint (Bu-yeon).....	55
Figure 5-9 Detail of the repaired member (bu-yeon)	56
Figure 5-10 Test set-up (Bu-yeon).....	57
Figure 5-11 The tusk tenon joint (Mok-gi-yeon).....	57
Figure 5-12 Detail of the repaired member (Mok-gi-yeon)	58
Figure 5-13 Test set-up (Mok-gi-yeon)	59
Figure 5-14 Load-Displacement curve (Chu-nyu)	60
Figure 5-15 Load-Displacement curve (Jang-yeon).....	61
Figure 5-16 Load-Displacement curve (Dan-yeon).....	61
Figure 5-17 Load-Displacement curve (Bu-yeon).....	62
Figure 5-18 Load-Displacement curve (Mok-gi-yeon)	62
Figure 5-19 Comparing the yield and the ultimate load.....	65
Figure 5-20 Comparing the stiffness	69
Figure 5-21 Comparing the ductility	73
Figure 5-22 Equivalent section of modified butt joint	75
Figure 5-23 Location of angle γ	77
Figure 5-24 Equivalent section of tusk tenon joint	79

Chapter 1. Introduction

1.1 Background

Traditional wooden structures account for 28% of the cultural assets designated by the country. Among them, national treasures account for 11% and treasures account for 89%. Over a long period of time, traditional wooden structures are damaged from various factors. Factors affecting damage include structural, environmental, chemical, and mechanical factors. The type of damage to the member varies depending on its location [1].

The aging traditional wooden structures are undergoing steadily repair work in accordance with 『the Cultural Heritage Protection Act』 . In the repair work of traditional wooden structures, it is common to replace damaged members with new members rather than repairing them. Korea's repair technology was focused on morphological research, and it was not enough to consider the repair of damaged members [2]. In order to use the existing members as much as possible by repairing and reinforcing damaged members, the 『Cultural Heritage Administration』 established evaluation criteria. In addition, the 『Korea Foundation for the Traditional Architecture and Technology』 was established as an affiliated organization, emphasizing the importance of repair technology for members.

Currently, various domestic studies are being conducted on the structural engineering field of traditional wooden structures. Representatively, there are

Chapter 1. Introduction

structural forms, structural analysis modeling, structural performance of joints, and repair, but the repair accounts for about 10%. Among them, the repair study was mainly the repair study of Chu-nyu using steel reinforcement [3].

There are no domestic related studies and guidelines for roof members other than Chu-Nyu. After visually checking the decay, reuse, surface treatment, and replacement of new materials are performed according to the degree of decay. Therefore, in this study, we intend to present data so that the existing members can be used to the maximum by establishing an appropriate structural model that can be applied to the repair of traditional wooden roofs.

1.2 Scope and Objectives

The purpose of this study is to present an appropriate repair plan for the roof member of a traditional wooden structures. There is a national interest in reusing the existing members of traditional wooden structures as much as possible. However, there have been relatively few related studies on small roof members. Therefore, the roof members of Jeongyodang Hall in Dosanseowon Confucian School, Lecture Hall of Sosu Confucian Academy, Yangjindang House, Namhansanseong Suengyeoljeon Hall were provided by 『Korea Foundation for the Traditional Architecture and Technology』 . The types of members are Chu-nyu, Yeon-mok, Bu-Yeon, and Mok-gi-yeon.

This paper proceeded as follows.

Structural analysis of the building was carried out based on the allowable stress design method (ASD). The roof load was calculated by referring to the repair report and actual measurement report of each structure. The calculated load was analyzed for the roof member through 『Midas Gen』 , a structural analysis program. Through the results, the safety of each member was reviewed, and structural vulnerable parts were identified.

Non-destructive diagnostic tests such as stress wave and drill resistance tests were used to investigate the cross-sectional state of the inside of the member. The residual strength test was compared with the result of the non-destructive diagnostic test. The applicability of the non-destructive diagnostic test was reviewed, and the decay of the actual member was identified.

Chapter 1. Introduction

According to the results of structural analysis and non-destructive diagnostic tests, the repair design was carried out by applying the applicable repair plan for the roof member. In consideration of the actual load, the experiment was conducted. The experimental results were analyzed through 『Midas Gen』 . As a result of the experiment, flexural strength, flexural stiffness, and ductility were calculated and compared with theoretical values. In addition, an equivalent sectional model was created and analyzed for comparison. Based on this, applicability was judged.

Chapter 2. Literature Review

2.1 Code Review

2.1.1 KS, KDS

There are two standards related to the repair of wooden structures. Standards for material properties are provided by KS (Korea Standards), and standards for design methods are provided by KDS (Korean Design Standard). The design uses Allowable stress design (ASD). There is a design method for mechanical joints, but there is no design method for traditional wooden joints. The Table 2-1 shows the standards of KS and KDS required for designing wooden joints.

Table 2-1 KS, KDS related to wooden joint

	Code number	Title
Material properties	KS F 2201: 2021	General requirements for testing of wood
	KS F 2206: 2020	Method of compression test for wood
	KS F 2207: 2020	Method of tension test for wood
	KS F 2208: 2020	Method of bending test for wood
	KS F 2209: 2020	Method of shear test for wood
Design Method -wooden structure	KDS 41 31 01: 2016	General information
	KDS 41 31 02: 2016	Material and allowable stress
	KDS 41 31 03: 2016	Design requirements
	KDS 41 31 04: 2019	Design of member
	KDS 41 31 05: 2016	Design of joints
	KDS 41 31 06: 2016	Traditional wooden structure

2.1.2 ISO

ISO (International Organization for Standardization) related to the repair of wooden structures provides three standards for wooden joints. The three standards provide experimental method for specimens to measure the strength and stiffness of wood joints. However, there is no standard for how to design a traditional joint. The Table 2-2 shows the ISO standards focusing on joints made with mechanical fasteners.

Table 2-2 ISO related to wooden joint

Code number	Title
ISO 6891:1983	Timber structures-joints made with mechanical fasteners-general principles for the determination of strength and deformation characteristics
ISO 8375:1985	Solid timber in structural sizes-determination of some physical and mechanical properties
ISO 8970:1985	Timber structures-testing of joints made with mechanical fasteners-requirements for timber density

2.1.3 ICOMOS

ICOMOS (International Council Monuments and Sites) presented 『The principle for the conservation of wooden built heritage』. According to this, a diagnosis should be made before the repair of traditional wooden structures. The diagnosis must be based on documentary evidence, physical inspection, and analysis and, if necessary, measurements of physical conditions using non-

destructive testing (NDT), and if necessary, on laboratory testing. In the repair work, it is specified to use the existing members as much as possible and follow the traditional repair technique. When replacing members, emphasize that the same type of wood should be used, and the moisture content should be similar.

2.2 Literature Review

2.2.1 Structural analysis of traditional wooden building

As shown in the Figure 2-1, Jo et al. [4] performed 2D and 3D structural analysis of the Muryangsujeon Hall of Buseoksa Temple, a traditional wooden structure, using 『SAP 2000』, a general structural analysis program. The size of the main structural members of the building was designed using the existing drawing data. The material properties of red pine, such as the wood used for the Muryangsujeon Hall, were applied. The load was calculated by considering the tile load and the soil load. As shown in the Figure 2-2, the supporting conditions were varied according to the condition of the joint.

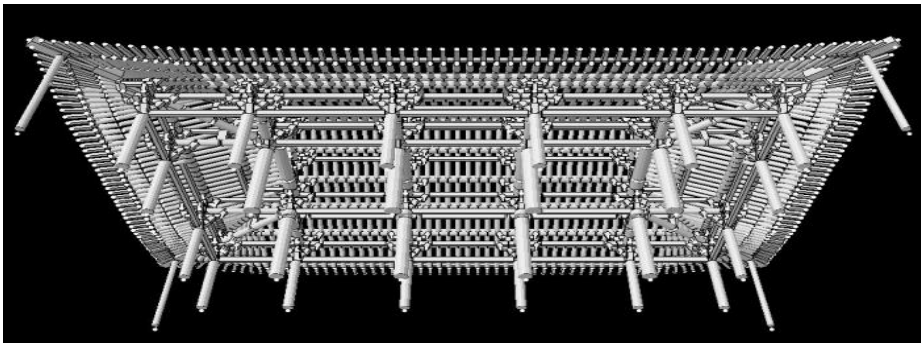


Figure 2-1 3D Modeling of Musangsujeon

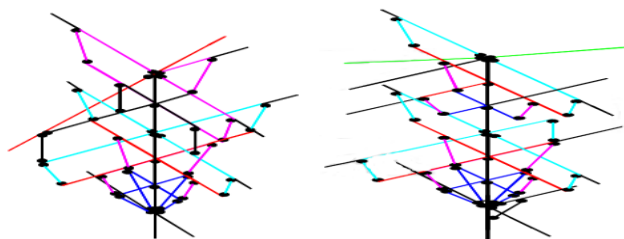


Figure 2-2 Modeling the support condition

As a result of the allowable stress analysis, there was little difference between the 2D and 3D structural analysis of the roof member. All Do-ri except for the Ju-sim Do-ri showed high shear stress. In the case of Yeon-mok, the bending stress was high, and in the case of the Bu-yeon, the shear stress was high. Most of the results were lower than the allowable stress, but Chul-mok Do-ri, Jang-yeon, Jang-yeo, and Cho-bang had higher than the allowable stress.

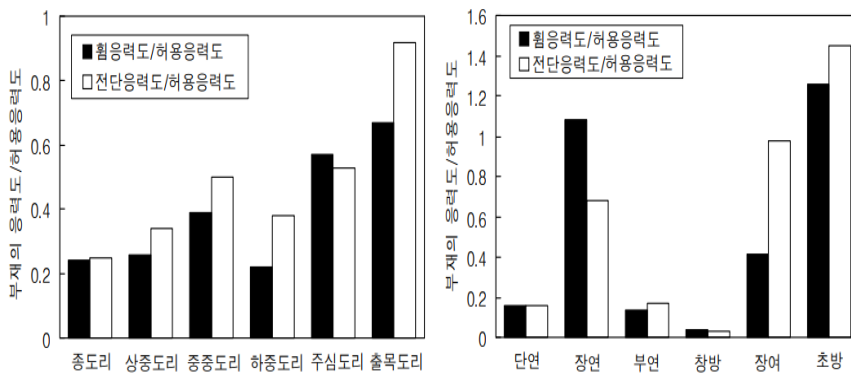


Figure 2-3 Allowable stress analysis result of roof member

2.2.2 Non-destructive diagnostic test

Lee et al. [5] performed non-destructive testing of wood (Figure 2-4) used in traditional wooden structures. Non-destructive testing of main structural members was conducted by ultrasonic stress wave test, drilling resistance test, and visual inspection. The internal cross section was identified through ultrasonic stress wave test and drilling resistance test. After that, the wood was cut and visually inspected.



Figure 2-4 The evaluated woods for NDT study

ultrasonic stress wave test and drilling resistance test were performed with an interval of 100mm (Figure 2-5). The drilling resistance test was carried out by moving 30 ° clockwise in the circular cross section. After the non-destructive test, the cross section was cut, and the visual inspection was performed. The results of visual inspection and non-destructive test were compared and analyzed.

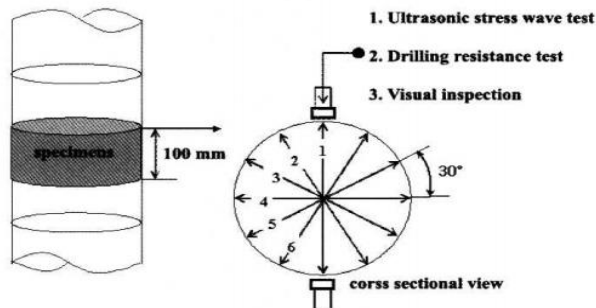


Figure 2-5 Measured positions of non-destructive testing in woods.

The correlation between the ultrasonic stress wave test and drilling resistance test was shown in the Figure 2-6. The cross section made based on the drilling resistance test result and the actual cross section are compared as shown in the Figure 2-7.

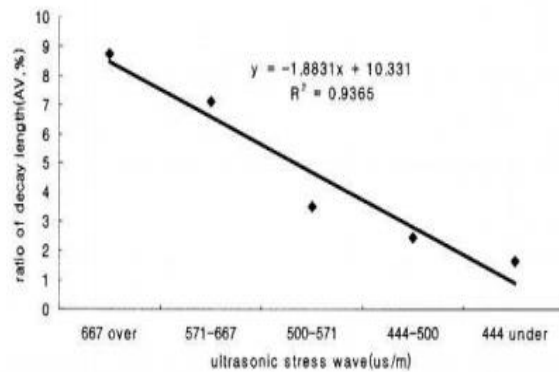


Figure 2-6 USW and ratio of decay length caused by DRT.

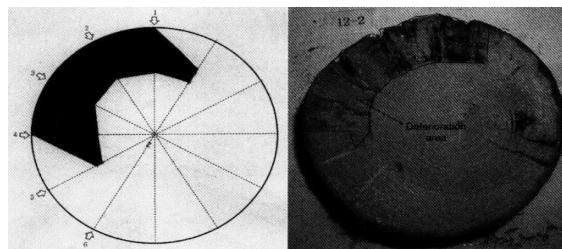


Figure 2-7 The comparison of artificial picture and real cross-section.

Comparing the results of the non-destructive test and the visual inspection, similar shapes were derived for the cross-sectional loss. Non-destructive testing can qualitatively determine the loss of a section and compare the loss of each section within the same member. To derive quantitative results, there are insufficient research results according to tree species, age, and moisture content. Therefore, there is a limit to evaluating the residual strength of a member only by non-destructive analysis.

2.2.3 The structural strengthening characteristic of Chu-nyu

Cho et al. [6] studied the reinforcement of Chu-nyu in a traditional wooden hipped-and-gabled roof. In his study, the upper part of the Chu-nyu was reinforced using carbon fiber bar. Based on Chu-nyu of Jinnamgwang Hall, the specimen was designed, and the experiment was performed.

As shown in the Figure 2-8, he analyzed the structural characteristics of Chu-nyu and calculated the reaction point, the loading point, and the load. The reinforcing section of Chu-nyu was reinforced by inserting two carbon fiber bars by digging a groove on the upper surface as shown in the Figure 2-9.

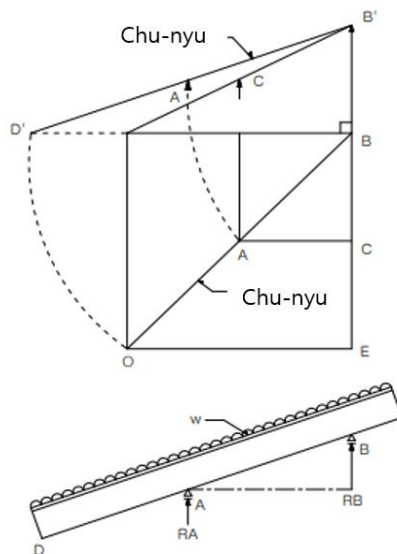


Figure 2-8 The slope of a roof and structural points of Chu-nyu

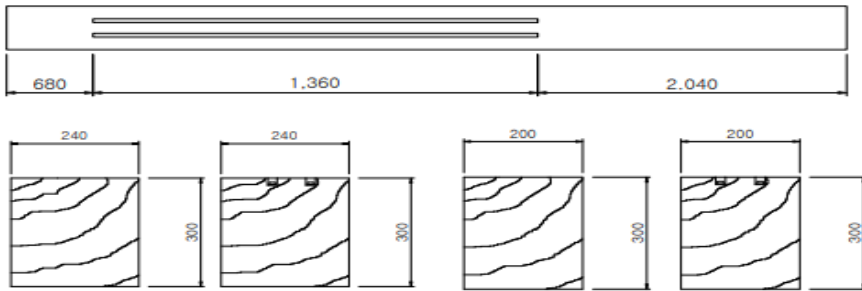


Figure 2-9 Elevation and section views of Chu-nyu

As shown in the Figure 2-10, the experiment was conducted by applying a concentrated load to two points, which are the locations where the actual roof load was concentrated, using the UTM(Universal Testing Machine) as shown in the figure. Displacement was measured by installing the LVDT(Linear Vertical Displacement Transducer) at the left end, right end, and middle of the reaction point.

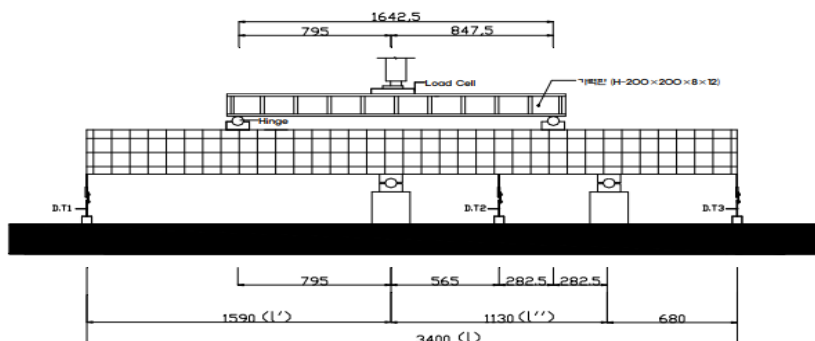


Figure 2-10 The experimental setup of Chu-nyu

Although there is a difference according to the ratio of the overhanging length, as shown in the Figure 2-11, the yield load and ultimate load of the

Chapter 2. Literature Review

reinforced specimen were overall increased compared to the reference specimen. As the overhanging length increased, the yield load decreased. As shown in the Figure 2-12, when the overhanging length was 1:1, the reinforced specimen increased, but as the overhanging length increased, it showed a tendency to become like that of the reference specimen.

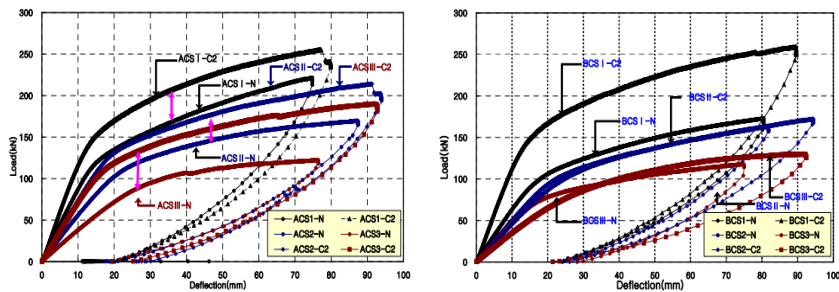


Figure 2-11 Comparison of load-deflection curves of specimens

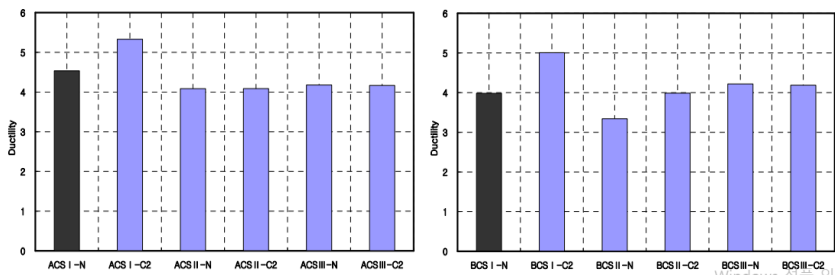


Figure 2-12 Comparison of ductility of specimens

In this study, it was designed considering the load condition of the Chu-nyu, and only the effect of the reinforcement and the overhanging length were considered. The actual Chu-nyu is the curved shape in Cheoma Do-ri, but the effect caused by this shape is not considered and there is a limit to its practical application.

Chapter 3. Structural analysis

3.1 Introduction

The members of traditional wooden structures are not uniform in cross section and have various load conditions. In particular, the roof member has a soil load and a roof tile load that are not uniformly distributed, and the position where the member is placed has a slope. Through structural analysis, the ratio of allowable stresses and vulnerable part of the roof members were identified.

Structural analysis of the gravity load was performed, and stability was reviewed for the structures of Jeongyodang Hall in Dosanseowon Confucian School, Lecture Hall of Sosu Confucian Academy, Yangjindang House, Namhansanseong Suengyeoljeon Hall. Vulnerable parts were identified for the roof member of the building. The 『Midas Gen』 program was used for the analysis. The analytic model applied major roof members such as Chu-nyu, Yeon-mok, Bu-yeon, Mok-gi-yeon. The properties of the material were applied to the properties of pine trees used in domestic traditional wooden structures. In the case of the joint, the end of the horizontal member was set as a pin-joint without bending resistance performance, and the lower end of the vertical member was assumed to be rigid-joint because it had bending resistance performance due to vertical load. The weight of the soil per unit volume (W_s) and the weight of tiles per unit area (W_t) were assumed as follows by referring to the related literature [7].

$$W_s = 16kN/m^3, \quad W_t = 2kN/m^2$$

3.2 Design allowable stress

The type of wood was assumed to be pine Grade 2 (lumber) [8], and the standard allowable stress and modulus of elasticity were determined according to Table 1.1-4 of 『Building Structural Standards-Wood Structural Materials and Allowable Stresses』 (KDS 41 33 02: 2016). For the modification factor for calculating the allowable stress, refer to Tables 1.1-6 to 1.1-11 of KDS 41 33 02. The allowable bending stress(F'_b) and allowable shear stress(F'_v) were calculated as follows by applying a modification factor to the standard allowable bending stress (F_b) and the standard allowable shear stress (F_v), respectively. At this time, the grade of pine trees was set to Grade 2.

$$\begin{aligned}
 F'_b &= F_b(C_D)(C_M)(C_t)(C_L)(C_f) \\
 &= 6.0 \times 1.15 \times 1.0 \times 1.0 \times 1.0 \times (C_f) \\
 &= 6.9\text{MPa} \times (C_f)
 \end{aligned}$$

$$\begin{aligned}
 F'_v &= F_v(C_D)(C_M)(C_t)(C_H) \\
 &= 1.1 \times 1.15 \times 1.0 \times 1.0 \times 1.0 = 1.27\text{MPa}
 \end{aligned}$$

Table 3-1 Standard allowable stress for visual grade structural members, which are conifers (KDS 41 33 02 Table 1.1-4)

Tree species classification		Grade	Standard allowable stress (unit : MPa)					
			F_b	F_t	F_c	$F_{c\perp}$	F_v	E
Species	Pine	1	7.5	5.0	7.5	3.0	1.1	10,300
		2	6.0	3.5	4.5	3.0	1.1	9,000
		3	3.5	2.0	3.0	3.0	1.1	8,300

Table 3-2 modification factor of allowable design stress (KDS 41 33 02 Table.1.1-6)

Design allowable stress	Standard allowable stress	Load period factor	Moisture factor	Temperature factor	Lateral factor ¹⁾	Dimension factor	Volumn factor ³⁾	Plane usage factor ⁴⁾	Repeat member factor ⁵⁾	Curvature factor ⁶⁾	Shape factor	Column stability factor	Shear stress factor	Buckling stiffness factor ⁷⁾	Acupressure area factor	Incising factor
$F_b \prime =$	F_b	C_D	C_M	C_t	C_L	C_F	C_v	C_{fu}	C_r	C_c	C_f	C_i
$F_t \prime =$	F_t	C_D	C_M	C_t	.	C_F	C_i
$F_v \prime =$	F_v	C_D	C_M	C_t	C_H	.	.	C_i
$F_{c\perp} \prime =$	$F_{c\perp}$.	C_M	C_t	C_b	C_i
$F_c \prime =$	F_c	C_D	C_M	C_t	.	C_F	C_p	.	.	.	C_i
$E =$	E	.	C_M	C_t	C_T	.	C_i
$F_g \prime =$	F_g	C_D	.	C_t

- Comment
- 1) For a lamination wood subjected to a flexural load, the lateral factor C_L and the volume factor C_v are not applied together, but the smaller of the two modification factors is applied.
 - 2) The dimensional factor C_F is applied only to visual grade structural members and circular section structural members subjected to bending loads.
 - 3) The volume factor C_v is applied only to the lamination wood subjected to the flexural load.
 - 4) The plane usage factor C_{fu} is applied only to class 1 structural materials (standard wood) and lamination wood that are subjected to bending loads.
 - 5) The repeat member factor C_r is applied only to class 1 structural members (standard wood) subjected to flexural loads.
 - 6) The curvature coefficient C_c is applied only to the bent part of the lamination wood subjected to the flexural load.
 - 7) The buckling stiffness coefficient C_T is applied only to the truss compression chords of small structural members of 38×89 mm or less. This regulation applies only when a plywood cover with a thickness of 9 mm or more is nailed to the top of a truss compression chord and is subjected to both bending and compressive stress in the fiber direction.

3.3 Structural analysis by member

3.3.1 Chu-nyu

Due to the characteristics of traditional wooden structures, the Chu-nyu is a nonlinear structure, and it is difficult to accurately calculate the loads of the Yeon-mok and Chu-nyu. Therefore, the load acting on the roof surface of the square area around the Chu-nyu was assumed to be supported by the Chu-nyu and calculated conservatively. The load on the square plane with the diagonal of the Chu-nyu was replaced with a linear load, and the load was applied in a triangular shape. The Chu-nyu of Jeongyodang Hall in Dosanseowon Confucian School, Lecture Hall of Sosu Confucian Academy, Yangjindang House can be approximated in the form of a simple beam with two reaction points at the Cheoma Do-ri and at Jung Do-ri. In the case of the Namhansanseong Suengyeoljeon Hall, there is no Chu-nyu with a gable roof. The roof load was assumed to be $7.5kN/m^2$ [7].

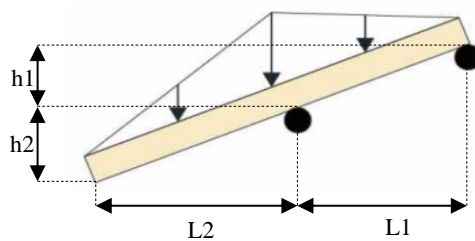


Figure 3-1 Length and height measurement for structural review of Chu-nyu

Table 3-3 Chu-nyu length and height measurement of each building

	Jeongyodang hall	Lecture Hall of Sosu	Yangjindang House
h1	604 mm	735 mm	382 mm
h2	671 mm	550 mm	147 mm
L1	2,107 mm	2,543 mm	2,089 mm
L2	2,343 mm	2,857 mm	1,847 mm

3.3.2 Yeon-mok

The load was considered Yeon-mok's self-weight and roof load. The roof load considered the weight of the roof tile and the weight of soil. As shown in Figure 3-2, it is assumed that the load is supported on the Do-ri as a point through the Yeon-mok in the form of a simple beam, and the load is applied to each of the Do-ri by calculating the reaction force. The soil load was assumed to be a linear distributed load, and the soil thickness ($h_1 \sim h_4$) (refer to Figure 3-3) and unit weight were assumed and reflected in the calculation.

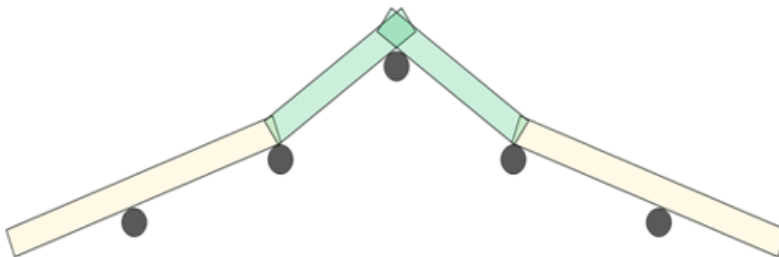


Figure 3-2 Example of Yeon-mok in the form of a simple beam

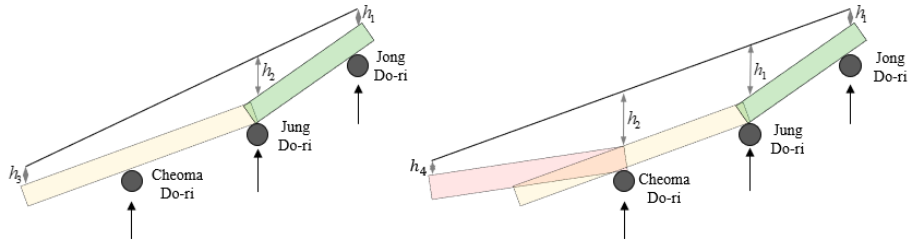


Figure 3-3 Location of $h_1 \sim h_4$ for calculation of soil thickness

Table 3-4 The soil thickness of each structure

	Jeongyodang Hall	Lecture Hall of Sosu	Yangjindang House	Suengyeoljeon Hall
h_1	340mm	330mm	480mm	300mm
h_2	480mm	410mm	600mm	580mm
h_3	180mm	320mm	150mm	420mm
h_4	-	210mm	-	200mm

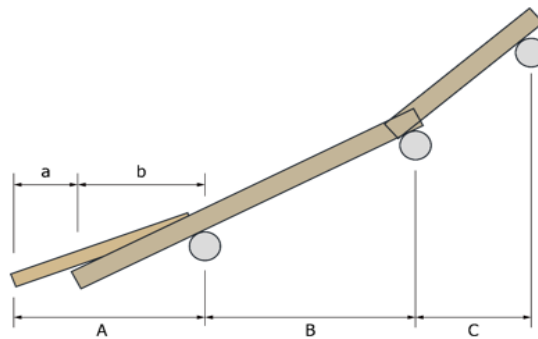


Figure 3-4 Model for measuring the horizontal length of Yeon-mok

Table 3-5 The horizontal length of each structure

	Jeongyodang Hall	Lecture Hall of Sosu	Yangjindang House	Suengyeoljeon Hall
A	1,440mm	1,740mm	1,500mm	1,350mm
B	1,470mm	1,850mm	1,530mm	1,900mm
C	1,020mm	1,410mm	1,240mm	925mm
a	-	550mm	-	450mm
b	-	1,190mm	-	900mm

3.3.3 Bu-yeon

It is only found in Lecture Hall of Sosu Confucian Academy and Namhansanseong Suengyeoljeon Hall, which are double eaves. Structural analysis was conducted by referring to the actual drawings of Lecture Hall of Sosu Confucian Academy and Namhansanseong Suengyeoljeon Hall. In the Yeon-mok structural analysis, the soil thickness (Table 3-4) and the horizontal length (Table 3-6) were used to calculate the soil load and tile load. Modeling was performed in the form of a simple beam that is the same as the actual condition of Bu-yeon. In the case of the root part, the cross section becomes smaller toward the edge. Bu-yeon is in contact with the upper surface of Yeon-mok from the part where the cross section becomes smaller to the edge.

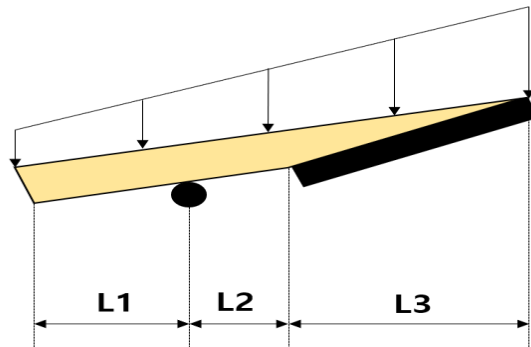


Figure 3-5 Calculation of reaction point for structural review of Bu-yeon

Table 3-6 Measuring of horizontal length of Bu-yeon

	L1	L2	L3
Lecture Hall of Sosu	550 mm	100 mm	900 mm
Suengyeoljeon Hall	450 mm	80 mm	720 mm

3.3.4 Mok-gi-yeon

Structural analysis was performed by referring to the actual drawings of Jeongyodang Hall in Dosanseowon Confucian School, Lecture Hall of Sosu Confucian Academy, Yangjindang House, Namhansanseong Suengyeoljeon Hall. The location of Mok-gi-yeon is on the gable board, and the load of gable ridge is concentrated on the head of Mok-gi-yeon. The roof tile load was calculated by calculating the number of tiles of the ridge. The expected load was conservatively calculated by referring to the design drawings and repair reports of each structure. The structural system has a free end on the outside

and is supported on the inside based on the gable board. Therefore, it becomes a cantilever beam type.

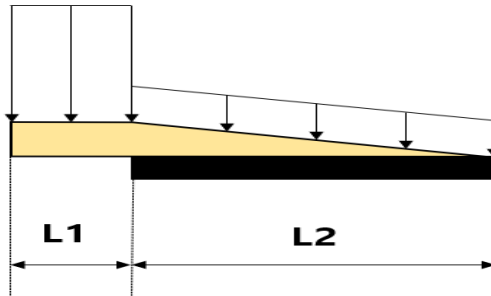


Figure 3-6 Model for measuring the horizontal length of Mok-gi-yeon

Table 3-7 The horizontal length of each structure

	B x H (mm²)	L1	L2	Gable ridge
Jeongyodang hall	75×95	150 mm	450 mm	3
Lecture Hall of Sosu	85×115	230 mm	1070 mm	3
Yangjindang House	90×110	240 mm	1100 mm	3
Suengyeoljeon Hall	90×120	240 mm	800 mm	3

3.4 Structural analysis results and discussion

By applying the load conditions and structural system analyzed in Chapter 3, the roof members of Jeongyodang Hall in Dosanseowon Confucian School, Lecture Hall of Sosu Confucian Academy, Yangjindang House, Namhansanseong Suengyeoljeon Hall were analyzed using 『Midas Gen』 (Table 3-8 ~ Table 3-11).

All members showed a result value lower than the allowable stress. Most of the members are less than 60% of the allowable stress, but only Jang-yeon calculated that the allowable stress ratio is higher than that of other members (Table 3-12).

Chu-nyu can see that the bending stress ratio is about 40%. The cross section of Chu-nyu is the largest among roof members. Chu-nyu can be divided into the head and the root. As a load is applied to the head and the root, bending moment and shear force occur most at the eaves. The structural weakness is the Cheoma Do-ri point.

Comparing Yeon-mok's Dan-yeon and Jang-yeon, Jang-yeon has a lot of bending moment and shear force. This is because the relatively long Jang-yeon is receiving more loads. Examining the allowable stress ratio, Yeon-mok has a greater bending stress. The vulnerable part of Dan-yeon is the central part where the bending moment is concentrated, and the vulnerable part of Jang-yeon is the Cheoma Do-ri where the most bending moment and shear force are applied.

Bu-yeon's allowable bending stress and allowable shear stress are less than

10%. The allowable shear stress is slightly higher. The weak point of Bu-yeon is near the Bu-yeon Chak-go where the bending moment and shear force are high.

Mok-gi-yeon has low bending stress ratio (maximum 2.48%) and shear stress ratio (maximum 4.09%). Unlike Chu-nyu and yeon-mok, Mok-gi-yeon has less area to receive loads. In Chu-nyu and yeon-mok, each member transmits the load to the Do-ri or column, but Mok-gi-yeon receives the load of a portion of the roof that touches the upper surface of the member, and the rest load does not go through Mok-gi-yeon. Due to its characteristics, it is difficult to conclude that it is a major structural member. The vulnerable part of Mok-gi-yeon is near the gable board point.

Chapter 3. Structural analysis

Table 3-8 Structural analysis results of Jeongyodang Hall

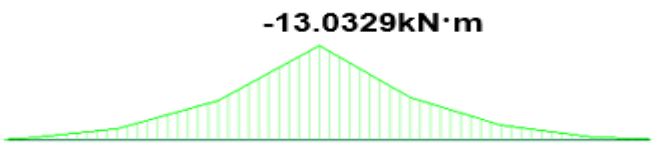
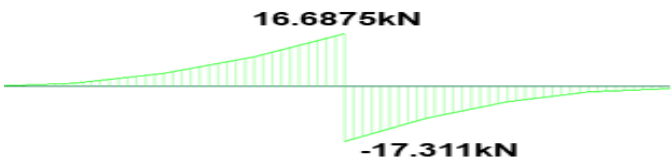
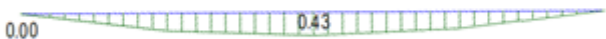

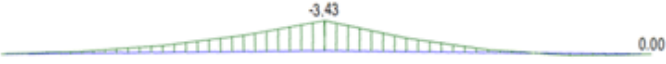
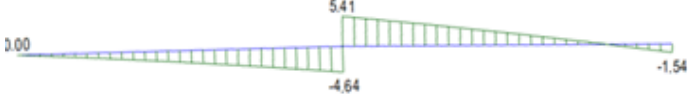
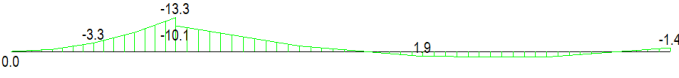
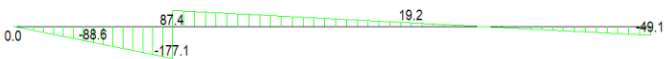
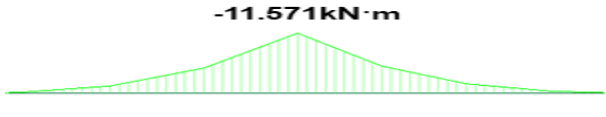
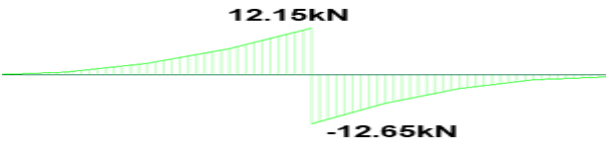
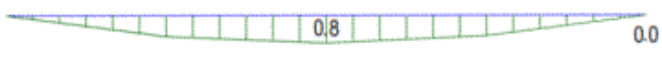


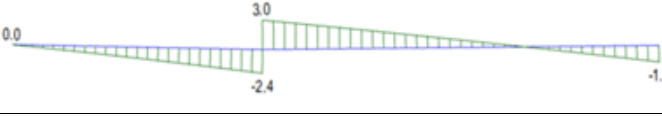


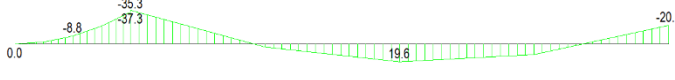
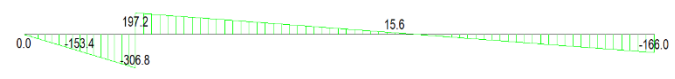
Chu-nyu	BMD (kN·m)	
	SFD (kN)	
Dan-Yeon	BMD (kN·m)	
	SFD (kN)	
Jang-yeon	BMD (kN·m)	
	SFD (kN)	
Mok-gi-yeon	BMD (N·m)	
	SFD (N)	

Table 3-9 Structural analysis results of Lecture Hall of Sosu

Chu-nyu	BMD (kN·m)	
	SFD (kN)	
Dan-Yeon	BMD (kN·m)	
	SFD (kN)	
Jang-yeon	BMD (kN·m)	
	SFD (kN)	
Bu-yeon	BMD (N·m)	
	SFD (N)	
Mok-gi-yeon	BMD (N·m)	
	SFD (N)	

Chapter 3. Structural analysis

Table 3-10 Structural analysis results of Yangjindang House

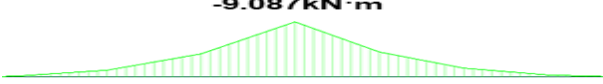
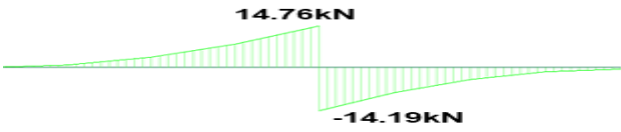
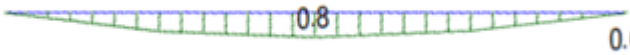


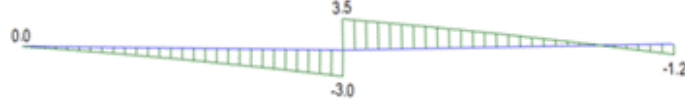
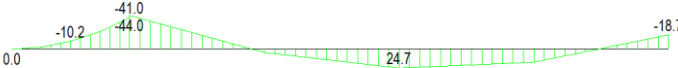
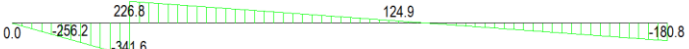
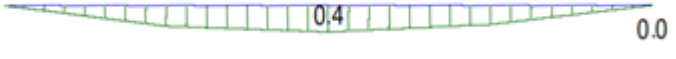

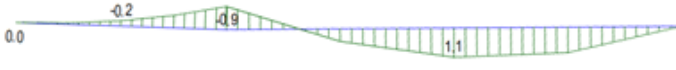
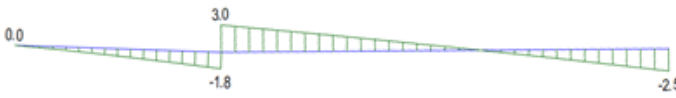
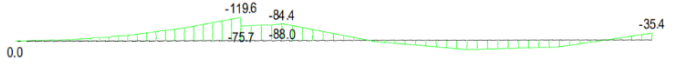
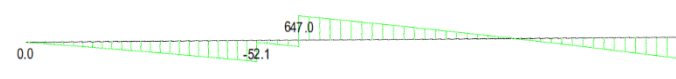
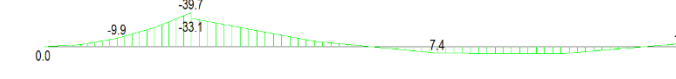
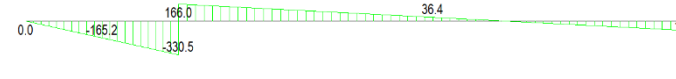
Chu-nyu	BMD (kN·m)	
	SFD (kN)	
Dan-Yeon	BMD (kN·m)	
	SFD (kN)	
Jang-yeon	BMD (kN·m)	
	SFD (kN)	
Mok-gi-yeon	BMD (N·m)	
	SFD (N)	

Table 3-11 Structural analysis results of Suengyeoljeon Hall

Dan-yeon	BMD (kN·m)	
	SFD (kN)	
Jang-yeon	BMD (kN·m)	
	SFD (kN)	
Bu-yeon	BMD (N·m)	
	SFD (N)	
Mok-gi-yeon	BMD (N·m)	
	SFD (N)	

Chapter 3. Structural analysis

Table 3-12 Result of Allowable stress ratio

		Maximum bending moment	Maximum bending stress	Allowable bending stress	Bending stress ratio	Maximum Shear Force	Maximum Shear Stress	Allowable shear stress	Shear Stress Ratio
Jeongyodang Hall	Dan-yeon	0.43 kN · m	1.30 MPa	8.14 MPa	16.0 %	1.40 kN	0.11 MPa	1.27 MPa	8.7 %
	Jang-yeon	3.43 kN · m	6.52 MPa	8.14 MPa	80.1 %	5.41 kN	0.30 MPa	1.27 MPa	23.6 %
	Chu-nyu	13.0 kN · m	4.13 MPa	9.76 MPa	42.3 %	17.3 kN	0.28 MPa	1.27 MPa	22.0 %
	Mok-gi-yeon	13.3 N · m	0.117 MPa	9.76 MPa	1.19 %	177.1 N	0.037 MPa	1.27 MPa	2.91 %
Lecture Hall of Sosu	Dan-yeon	0.8 kN · m	4.17 MPa	8.14 MPa	51.2 %	1.8 kN	0.20 MPa	1.27 MPa	15.7 %
	Jang-yeon	1.5 kN · m	6.21 MPa	8.14 MPa	76.3 %	3.0 kN	0.28 MPa	1.27 MPa	22.0 %
	Chu-nyu	11.6 kN · m	3.82 MPa	9.76 MPa	39.1 %	12.65 kN	0.29 MPa	1.27 MPa	22.8 %
	Bu-yeon	218.2 N · m	0.782 MPa	9.76 MPa	8.18 %	938.7 N	0.116 Mpa	1.27 MPa	9.13 %
	Mok-gi-yeon	37.3 N · m	0.199 MPa	9.76 MPa	2.04 %	306.8 N	0.047 Mpa	1.27 MPa	3.70 %
Yangjindang House	Dan-yeon	0.8 kN · m	4.72 MPa	8.14 MPa	58.0 %	2.1 kN	0.20 MPa	1.27 MPa	15.7 %
	Jang-yeon	2.1 kN · m	7.80 MPa	8.14 MPa	95.8 %	3.5 kN	0.30 MPa	1.27 MPa	23.6 %
	Chu-nyu	9.1 kN · m	3.16 MPa	9.76 MPa	32.4 %	14.8 kN	0.36 MPa	1.27 MPa	28.3 %
	Mok-gi-yeon	44.0 N · m	0.242 MPa	9.76 MPa	2.48 %	341.6 N	0.052 MPa	1.27 MPa	4.09 %
Suengyeoljeon Hall	Dan-yeon	0.4 kN · m	1.66 MPa	8.14 MPa	20.4 %	1.3 kN	0.12 MPa	1.27 MPa	9.4 %
	Jang-yeon	1.1 kN · m	4.55 MPa	8.14 MPa	55.9 %	3.0 kN	0.28 MPa	1.27 MPa	22.0 %
	Bu-yeon	119.6 N · m	0.554 MPa	9.76 MPa	5.68 %	647.0 N	0.090 MPa	1.27 Mpa	7.09 %
	Mok-gi-yeon	39.7 N · m	0.184 MPa	9.76 MPa	1.89 %	330.5 N	0.046 MPa	1.27 MPa	3.62 %

Table 3-13 vulnerable part of roof member

	Bending Moment diagram	Shear force diagram	Vulnerable part
Chu-nyu	<p>-13.0329kN·m</p>	<p>16.6875kN -17.311kN</p>	Cheoma Do-ri
Dan-yeon	<p>0.8</p>	<p>1.8 -1.7</p>	Center
Jang-yeon	<p>1.5</p>	<p>3.0 -2.4</p>	Cheoma Do-ri
Bu-yeon	<p>218.2 198.5 191.0 188.4 16.1</p>	<p>98.7 96.8</p>	Bu-yeon Chak-go
Mok-gi-yeon	<p>44.0 41.0 24.7 18.7 10.2</p>	<p>226.8 124.9 180.8 258.2 341.6</p>	Gable Board

Chapter 4. Non-destructive diagnostic test of damaged member

Experimental members (2 Chu-nyu, 18 Yeon-mok, 2 Bu-yeon, and 5 Mok-gi-yeon) were provided in 『Korea Foundation for the Traditional Architecture and Technology』. The experimental members were dismantled at Jeongyodang Hall in Dosanseowon Confucian School, Lecture Hall of Sosu Confucian Academy, Yangjindang House.

Members dismantled from traditional wooden structures are characterized by large sizes, non-uniform shapes, and uneven surface appearance. The deterioration was diagnosed by applying the wood non-destructive diagnostic test to these dismantled members, and it was examined whether significant results could be derived.

4.1 Non-destructive diagnostic test

Non-destructive analysis methods for evaluating the internal deterioration of traditional wooden structures include elastic wave (stress wave, ultrasonic, etc.) test, drill resistance test, and X-ray test. The evaluation of deterioration of the interior of the wooden member of a traditional wooden structure can be divided into qualitative and quantitative evaluation according to the method. To evaluate the residual strength due to deterioration, the residual strength of the member must be predicted based on a quantitative evaluation. It is considered

more efficient to first evaluate the deterioration qualitatively inside the member, and then to diagnose deterioration by quantitatively evaluating the deterioration of a certain size or more.

It is necessary to change the application method step by step in consideration of material characteristics such as inhomogeneity and anisotropy of wood. That is, the presence or absence of deterioration was determined using elastic waves, and the approximate magnitude of deterioration was determined by the drill resistance test in the presence of deterioration. The deterioration state is finally evaluated from the evaluation results obtained for each method by applying the non-destructive diagnostic testing method. In this study, among the non-destructive diagnostic testing methods, we intend to use the test method using the stress wave test and the drill resistance test in consideration of the field applicability that can be used conveniently in the field.

4.1.1 Stress wave test

1) Device specifications

Using Metriguard's 239A model, the stress wave transmission time through the specimen was measured. This device consists of a hammer that generates a stress wave, a detector that detects the stress wave, and a main body that measures and displays the time when the stress wave generated from the hammer reaches the detector.



Figure 4-1 Stress wave measuring device (Metriguard 239A)

2) Experimental method

As shown in Figure 4-2, the original sphere (bottom of the column) of the dismantling member was set as 0, and the reference line was set in the longitudinal direction. The measurement was started from a position 150 mm away from the lower part in the longitudinal direction, and measurements were taken with 300 mm in the longitudinal direction. For the member of the circular cross section, a stress was applied to the reference line, and the time during which the stress wave was transmitted from the opposite side was measured. In addition, the stress was applied at a point perpendicular to the reference line and the time at which the stress wave was transmitted from the opposite side was also measured. Measurements were made five times at the same location, and the average value excluding the highest and lowest values was used as the time through which the stress wave penetrated. The distance through which the stress wave was transmitted was measured, and the measured distance was divided by the time at which the stress wave was transmitted to derive the stress

wave transmission speed. The stress wave transmission speed was obtained by the following equation.

$$\text{Stress wave transmission speed(m/s)} = \frac{\text{stress wave transmission distance(m)}}{\text{stress wave transmission time(s)}}$$

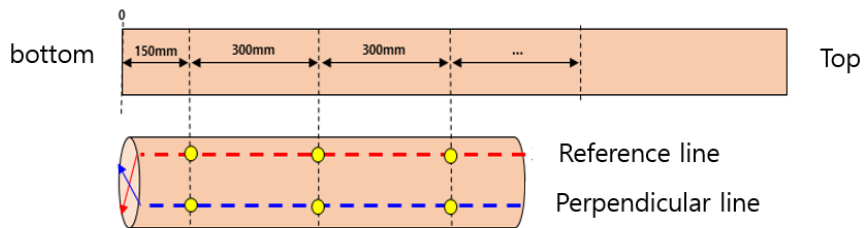


Figure 4-2 Stress wave test method

4.1.2 Drill resistance test

1) Device specifications

IML's F500-S model was used to measure the resistance force generated while the drill blade of the testing machine passed through the damaged member. A drill blade having a diameter of 3 mm and a length of 500 mm was used, and the experiment was conducted by selecting the tree species as softwood in the setting of the experimental device.

2) Experimental method

From the results of the stress wave test, the drill resistance test was performed on the cross section with a stress wave transmission speed of 500 m/s or less.

Chapter 4. Non-destructive diagnostic test of damaged member

The drill resistance test was carried out at the same position as the measured position of the stress wave test. If it is judged that there is internal deterioration, to diagnose the internal condition, measure 8 times at 22.5 degree intervals on the same cross-section as shown in Figure 4-4. CT images of the cross section were constructed using the Matlab program. The internal deterioration was estimated by displaying the areas with high and low drill resistance in different colors. Low drill resistance values are expressed in yellow (approximately 10% or less), high drill resistance values are expressed in blue (approximately 50% or more), and black parts indicate normal wood.



Figure 4-3 Drill resistance device (IML F500-S)

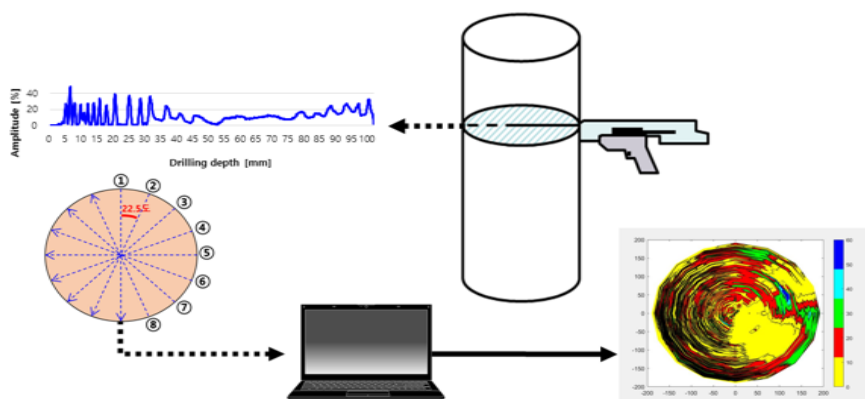


Figure 4-4 Drill resistance test

4.1.3 Non-destructive diagnostic test results (Refer to Appendix. A)

1) Chu-nyu

Chu-nyu is a member with a relatively large cross-section with a depth of about 300 mm. In the case of surface deterioration of these members, when visually inspected, a state in which the cross section was separated from the original surface to a depth of about 40 mm due to decay was seen. However, since it is not possible to visually inspect how much surface decay has progressed or penetrated the interior, stress wave tests and drill resistance tests were performed to check the internal decay state. This internal deterioration state of the member is closely related to the residual strength of the member and is intended to be used as a criterion for determining whether to reuse the member according to the residual strength of the member.

Among roof members, members with relatively large cross-sections often support relatively large loads. Therefore, if judging only by the deterioration state visible on the surface, there is a very high possibility of erroneous judgment of re-use, so it is necessary to understand the deterioration state of the inside of the member more accurately.

Chu-nyu showed initial decay to a depth of about 40 mm in addition to surface decay. In addition, the initial decay state of the interior cannot be detected by the stress wave test but can be detected only by the drill resistance test. This is because the initial decay state is a state in which the weight reduction rate is less than about 20%, so there is a high possibility that it cannot be detected by the stress wave test. In general, it is known that when the weight reduction rate is 20%, the strength reduction rate reaches about 50%.

Chapter 4. Non-destructive diagnostic test of damaged member

2) Yeon-mok

In the case of Jang-yeon and Dan-yeon, deterioration is generally observed on a part of the surface rather than the entire surface. Most of the stress wave test results of these members show that the stress wave transmission speed is 500 m/s or more, which is standard value, and the drill resistance test results for the inside of the member are also normal. In other words, it is judged that the decay that occurred in the central part of Yeon-mok has not progressed or penetrated further inside. However, in some members (Yangjindang House Jang-yeon 1, 7), the depth of surface decay was observed to be slightly deeper than that of other members, and the drill resistance test results for these members showed that there was a part judged to be an initial decay state inside. . In other words, depending on the condition of the surface decay, it can be seen that the decay has progressed inside.

On the other hand, at the edge of Yeon-mok, it is easy to permeate moisture through the end surface, so decay is easy to occur. Although the stress wave test results for this part were found to be in a healthy state, because of conducting the drill resistance test, the results were judged to be internal decay or initial decay.

3) Bu-yeon

In appearance, Bu-yeon 1 showed severe decay in the unpainted part (about 600mm from the left end). The stress wave test was performed in the direction perpendicular to the reference plane at positions 600 and 900 mm from the left

end with severe decay. The stress wave test was not possible at 300mm, so only the drill resistance test was performed. The stress wave transmission speed was 545 ~ 1,000 m/s, which exceeded the standard for decay judgment and was judged to be sound. The drill resistance test result is judged to have decayed from the surface to a depth of about 30 mm. This corresponds to 1/3 of the member depth. From the results of the non-destructive test, this member has a total length of about 1,000 mm, and decay occurred from the end face to 1/3 of the cross section. About 1/3 of the length is judged to be in a state of severe surface deterioration even by visual inspection, so it is judged that the replacement of the member is necessary.

The Bu-yeon 2 appeared to be in near good condition not long after it was replaced. The stress wave test was performed in the direction perpendicular to the reference plane at positions 300, 600, and 900 mm from the left end, respectively, and the result was a stress wave transmission speed of 1,058 ~ 1,384 m/s, indicating that the member was in good condition. .

4) Mok-gi-yeon

In appearance, slight decay was observed on some surfaces of the whole member, but overall it was observed to be in good health. The stress wave test was performed at the positions shown in the figure for all members (Appendix. A.). As a result of the stress wave test, the stress wave transmission speed at all measurement locations was 700 m/s or more, indicating that it was in a healthy state. When looking at the results of visual inspection and stress wave test, it was judged that all members were in a healthy state, so the drill resistance test was not conducted.

Chapter 4. Non-destructive diagnostic test of damaged member

Table 4-1 Dismantling member experiment detail

Structural	member	Section (mm)		length (mm)	Non-destructive		Bending test
		width	height		Stress wave	Drill resistance	
Lecture Hall of Sosu	Jang-Yeon1	Ø175		3,500	O	X	O
	Bu-yeon1	90	90	1,110	O	O	X
	Bu-yeon2	90	90	1,210	O	X	X
Jeongyodang hall	Chu-nyu1	205	300	5,480	O	O	O
	Chu-nyu2	205	300	5,300	O	O	O
	Jang-yeon1	Ø145		3,410	O	X	O
	Jang-yeon2	Ø140		3,185	O	X	O
Yangjindang House	Dan-yeon1	Ø151		1,820	O	O	O
	Dan-yeon2	Ø170		1,877	O	O	O
	Dan-yeon3	Ø166		1,797	O	O	O
	Dan-yeon4	Ø116		1,802	O	X	O
	Dan-yeon5	Ø149		1,834	O	O	O
	Jang-yeon1	Ø135		4,150	O	O	O
	Jang-yeon2	Ø135		3,165	O	X	O
	Jang-yeon3	Ø135		3,164	O	O	O
	Jang-yeon4	Ø137		3,674	O	O	O
	Jang-yeon5	Ø132		3,154	O	O	O
	Jang-yeon6	Ø135		3,175	O	O	O
	Jang-yeon7	Ø133		3,128	O	O	O
	Jang-yeon8	Ø130		3,160	O	X	O
	Jang-yeon9	Ø136		3,008	O	X	O
	Jang-yeon10	Ø178		3,505	O	X	O
	Mok-gi-yeon1	85	115	1,390	O	X	X
	Mok-gi-yeon2	93	110	1,300	O	X	X
	Mok-gi-yeon3	82	125	1,446	O	X	X
	Mok-gi-yeon4	87	114	1,238	O	X	X
	Mok-gi-yeon5	88	118	919	O	X	X

4.2 Residual strength experiment

As it is a roof member, it was determined that the loads received by the members would be mainly flexural loads, and a flexural test was performed to evaluate the residual strength of the flexural strength of the members based on the quantitative evaluation results of deterioration obtained by non-destructive diagnostic testing. In addition, only Yeon-mok's flexural test was conducted. Since Yeon-mok has a simple shape, it is relatively easy to predict the results of non-destructive testing and residual strength compared to other members.

1) Device specifications

The whitening experiment was performed using a universal strength tester (manufactured by Zwick, maximum load 10kN). The test conditions of Yeon-mok were crosshead speed 5mm/min, span was 3,000mm, 2,400mm, and 1,600mm depending on the length of the test piece, and the load condition was centralized load, and the support condition was simple support.



Figure 4-5 Flexural test

Chapter 4. Non-destructive diagnostic test of damaged member

2) Experimental method

According to the results of previous studies, it has been found that moment of inertia of the sound section excluding the defective section of the section is a remarkably effective factor in evaluating the flexural residual strength. Therefore, the residual flexural strength is evaluated using the moment of inertia as a major influence factor.

Table 4-2 Bending test result of Yeon-mok

	member	Diameter (mm)	I ($\times 10^6$ mm)	P _m (kN)	MOR (MPa)	MOE (GPa)	Form of destruction
Lecture Hall of Sosu	Jang-yeon	Ø185	57.60	44.66	53.9	6.7	Normal
Jeongyodang hall	Jang-yeon1	Ø145	21.70	21.32	53.4	9.8	Normal
	Jang-yeon2	Ø170	41.00	33.30	51.8	7.3	Normal
Yangjindang House	Dan-yeon1	Ø155	28.30	35.59	38.9	3.6	Shear fracture
	Dan-yeon2	Ø160	32.17	53.56	53.3	3.8	Normal
	Dan-yeon3	Ø160	32.17	33.04	32.9	2.9	Brittle fracture
	Dan-yeon4	Ø120	10.18	16.20	38.2	5.8	Brittle fracture
	Dan-yeon5	Ø145	21.70	35.21	47.1	4.0	Brittle fracture
	Jang-yeon1	Ø150	24.85	28.11	63.6	8.8	Normal
	Jang-yeon2	Ø150	24.85	29.39	66.5	11.2	Normal
	Jang-yeon3	Ø160	32.17	26.73	49.9	6.0	Brittle fracture
	Jang-yeon4	Ø150	24.85	25.84	58.5	9.1	Brittle fracture
	Jang-yeon5	Ø150	24.85	34.48	78.1	14.8	Normal
	Jang-yeon6	Ø155	28.33	28.49	58.5	8.9	Normal
	Jang-yeon7	Ø150	24.85	17.76	40.2	5.8	Normal
	Jang-yeon8	Ø155	28.33	22.19	45.5	8.8	Normal
	Jang-yeon9	Ø160	32.17	46.19	68.9	8.3	Normal
Jang-yeon10	Ø150	24.85	35.17	63.7	7.6	Normal	

4.3 Conclusion

The fracture mode was 'normal', indicating a general bending fracture of wood, 'brittle fracture' rather than a general fracture type, and 'shear fracture' occurred near the support point.

Looking at the results of the flexural test according to the fracture type, normal fracture occurred in 13 specimens, and the flexural strength of these specimens was 40.2 ~ 78.1 MPa. The average of these values is 58.14 MPa. This value represents a larger value than the 7.4 MPa value corresponding to pine grade 1 in the standard allowable stress of visually graded structural materials presented in National Institute of Forest Science Notification No. 2016-8 (Standards and Quality Standards for Wood Products). That is, among the members used in the flexural test, the members showing normal failure are strength-appropriate for reuse.

Also, looking at the flexural modulus of the above specimen, Dan-yeon 2 of Yangjindang House contains circular segments on the cross section of the member. Due to this, the dimensions of the actual cross-section are reduced, and the flexural modulus is 3.8 GPa, indicating a very small value despite the normal fracture shape. Jang-yeon 1 of Yangjindang House showed some signs of internal decay as a result of the drill resistance test, but the flexural modulus was found to be almost normal at 8.8 GPa. Jang-yeon 7 of Yangjindang House was judged to have signs of internal decay from the drill resistance test result, and the flexural modulus was also low at 5.8 GPa. In this member, the flexural strength showed a low value of 40.2 MPa even though failure occurred in the

normal fracture mode. The other members showed values of 6.7 ~ 14.8 GPa, and it can be said that the effect of surface decay or initial decay on the flexural modulus is greater than the flexural strength.

In the case of a member showing brittle fracture, the flexural strength is 32.9, 38.2, and 47.1 MPa, respectively. These values correspond to the first grade of structural lumber, but in terms of flexural modulus, 2.9, 5.8, and 4.4 GPa, respectively. These values are structural members was found to be unsuitable for use. However, it is judged that a more detailed examination is necessary for the cause of such brittle fracture.

Summarizing the above results, when the members used in this experiment show normal failure, they maintain sufficient strength in terms of strength. The flexural modulus shows an unsuitable value for use depending on the decaying state of the surface and the initial decaying state of the interior, so it is necessary to review the standard for this. Even in the case of a member showing brittle fracture, the flexural strength maintains a usable strength value, but the flexural modulus shows a value that cannot be used, so it is judged to be unsuitable for reuse. However, it is considered that further examination is necessary to set the standard for which such brittle fracture can be expected to occur.

Chapter 5. Repair design and experiments

Through structural analysis in Chapter 3, the structural vulnerable part of the roof member was identified. In Chapter 4, we identified the actual decay-vulnerable parts in the structural through visual and non-destructive diagnostic tests. Based on these two results, it was referred to in the investigation of the repair plan for the vulnerable. Repair cases in Korea were investigated and applicable repair designs were adopted.

5.1 Repair design and experiment.

5.1.1 Material property

Traditional wooden structures have been around for a long time, so there are some differences, but they are completely dry. However, the pine tree for the test specimen was not completely dried. To evaluate the quantitative structural safety of an actual structure and replace the member, it is an ideal approach to experiment with the member of the same species and age as the actual structure. However, it is practically impossible to obtain such members designated as cultural structure. Therefore, structural tests are conducted by evaluating the allowable stress of new wood, which is a pine family. The strength and mechanical properties of wood to be used in the roof member test are shown in the Table 5-1. Compared with the allowable stress specified in Korean Building Code, it is evaluated as a pine tree grade 1 or higher structural member, so it is appropriate as a member of the test. A titanium rod was used as a shear connection material for the Chu-nyu. Because titanium has high corrosion

Chapter 5. Repair design and experiments

resistance, it is suitable as a shear connector for wooden structures that are vulnerable to moisture. The mechanical properties of titanium to be used as shear connectors are shown in the Table 5-2. The distance according to the diameter of the titanium shear connector was calculated according to the Korean Building Code (Table 5-3).

Table 5-1 Wood (KS F 2206,2208,2209)

Tree species	Compressive stress	Bending stress	Shear stress	Modulus of elasticity	Moisture content
pine	27.2 MPa	46.6 MPa	8.7 MPa	10 GPa	17.2%

Table 5-2 Titanium bar

Grade	Yield strength	Tensile strength	Modulus of elasticity
2	275 MPa	345MPa	103 GPa

Table 5-3 The distance according to the diameter of the titanium shear connector

Diameter (mm)	Dowel bearing stress	Number of lines	Maximum interval (mm)	Minimum interval (mm)	Minimum edge distance (mm)	Minimum end distance (mm)	Minimum penetration depth (mm)
10	6.6 Mpa	2	160	50	40	70	80
15	12.4 Mpa	2	300	75	60	105	120
20	19.0 Mpa	2	450	100	80	140	160

Refer to KDS 41 33 05- 1.5.5.3 ~1.5.5.5, 1.7.3

5.1.2 Chu-nyu

1) Repair introduction

Chu-nyu is the member that receives the most load among the roof members and has the largest size. In Chapter 3 Structural Analysis, Chu-nyu showed a high bending stress ratio at the Cheoma Do-ri. As for the decay characteristics of the Chu-nyu, rainwater seeps in from the upper part of the joint between the Cheoma Do-ri and the Chu-nyu, so that the upper surface of the central part becomes decay and expands to the lower part. The cross section where the stress of the Chu-nyu is concentrated is lost and the fracture occurs. The existing repair method improved the performance by increasing the cross section through the addition of new material on the upper part of the decayed part. It is difficult to preserve the original shape of the structure due to the increase in section height h . This experiment tries to figure out the flexural performance of the member filled with new material after removing the decayed part.

2) Repair design

The reference member (Figure 5-1) and the repaired member(Figure 5-2) were manufactured based on Chu-nyu of Jeongyodang Hall in Dosanseowon Confucian School (width b : 200mm). The decay of Chu-nyu of Jeongyodang Hall was confirmed to be about 80mm from the upper surface. When manufacturing the repaired member, it was assumed that this part was removed to insert the backing wood. The backing wood was made with a thickness of 80 mm.

Shear flow (f) at the center of the cross section of Chu-nyu was calculated from the maximum shear force (17.3kN) applied to Chu-nyu resulting from the structural analysis.

$$f = \frac{3V}{2h} = \frac{3 \times 17,311\text{N}}{2 \times 300\text{mm}} = 86.5\text{N/mm}$$

Determination of allowable shear strength (F) and spacing (s) of shear connectors that satisfy the following equation.

$$f \leq \frac{F}{s}$$

The shear connectors of the repaired member were applied conservatively based on the calculated values and Table 5-3.

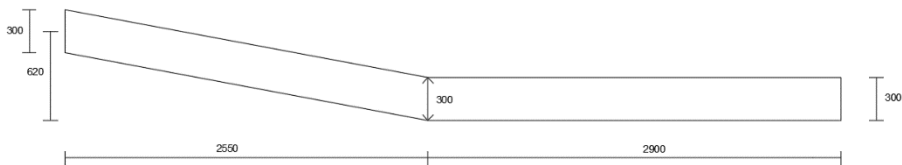


Figure 5-1 Detail of the reference member (Chu-nyu)

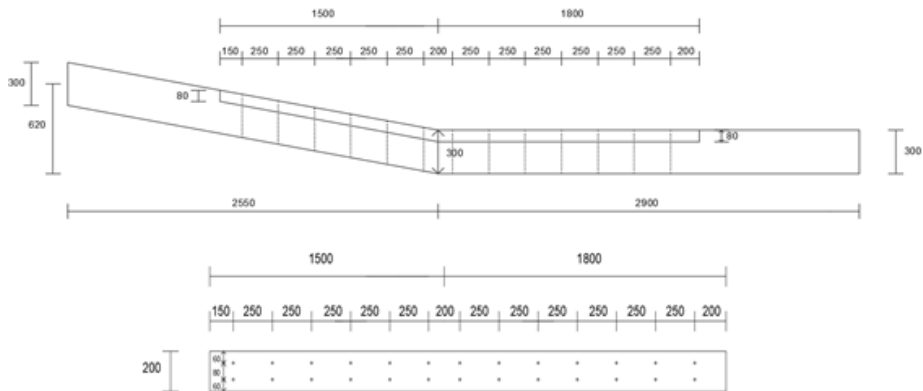


Figure 5-2 Detail of the repaired member (Chu-nyu)

After making a hole of 14 mm in the repaired member, the titanium bar (Diameter: 15 mm, Length: 30 cm) was inserted by hitting it with a hammer (Figure 5-3).



Figure 5-3 Titanium bar and inserting process

3) Experiment

The end of the specimen was set to support the root part like an actual Gang-da-ri or Chu-nyu-jeong, so, 500 mm of the root part was fixed with a steel jig as shown in the Figure 5-4, like the end condition. The reaction point was placed on the Jung Do-ri point and the Cheoma Do-ri. The distance between the

reaction points was set to 2,400 mm, and the distance between the loading points was set to be 1,500 mm. The loading was performed with a 150-ton actuator, and the loading speed was performed at 3 mm/min.

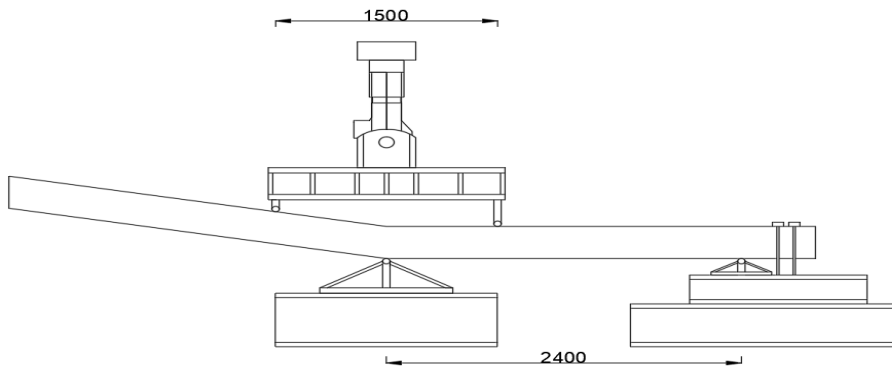


Figure 5-4 Test set-up (Chu-nyu)

5.1.3 Yeon-mok

1) Repair introduction

The Yeon-mok of Jeongyodang Hall in Dosanseowon Confucian School, Lecture Hall of Sosu Confucian Academy, Yangjindang House, Namhansanseong Suengyeoljeon Hall mainly have unbalanced decay of the upper surface, decay of the ends, and cracks in members. In the case of non-reusable members, after cutting the problematic part, a modified butt joint can be applied as shown in the Figure 5-5. In this experiment, Yeon-mok were designed by considering the ratio of the butt joint between Ha-jung Do-ri used in the Daejeokgwangjeon Hall of the Gwisinsa Temple. This experiment tries to figure out the bending performance of the designed Yeon-mok.

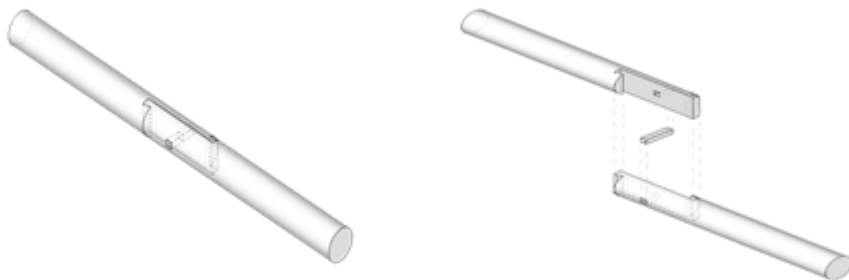


Figure 5-5 The modified butt joint

2) Repair design

The sizes of the reference member and the repaired member of Yeon-mok were produced with the average of the members provided by the foundation. The diameter was 150mm, the Jang-yeon's length was 3m, and the Dan-yeon's length was 2m. For the repaired member, referring to the actual measurement

drawings, a straight tenon was produced as much as $2/3$ of the radius, and the straight tenon was changed to the form of a rake. The joint length of the repaired member was set to 400 mm, and the length of the tenon groove was set to $1/10$ the joint length. The member of the Daejeokgwangjeon Hall was reinforced with steel nails to prevent slipping in the center part of the side. When the lower surface is exposed to the ceiling, a square wooden nail ($30\text{mm}\times 30\text{mm}$) was inserted in the actual experiment in consideration of the aesthetics of traditional wooden structure. (Figure 5-6)

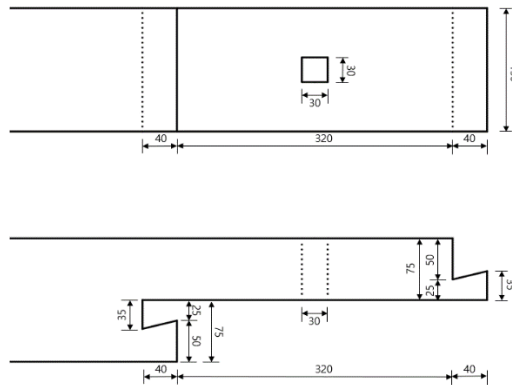


Figure 5-6 Detail of the repaired member (Yeon-mok)

3) Experiment

The members of Yeon-mok were 3000mm (Jang-yeon) and 2000mm (Dan-yeon). The reaction point was placed 100mm inside each end, and the distance between the reaction points was 2800mm and 1800mm. The loading was carried out in a three-point flexural test using a 10-ton UTM, and the loading speed was 5 mm/min, the same as in the flexural test of the Non-destructive

Chapter 5. Repair design and experiments

test. Since the cross section of the Yeon-mok is circular, a support for preventing fall was installed at a distance of 200 mm from the center (Figure 5-7).

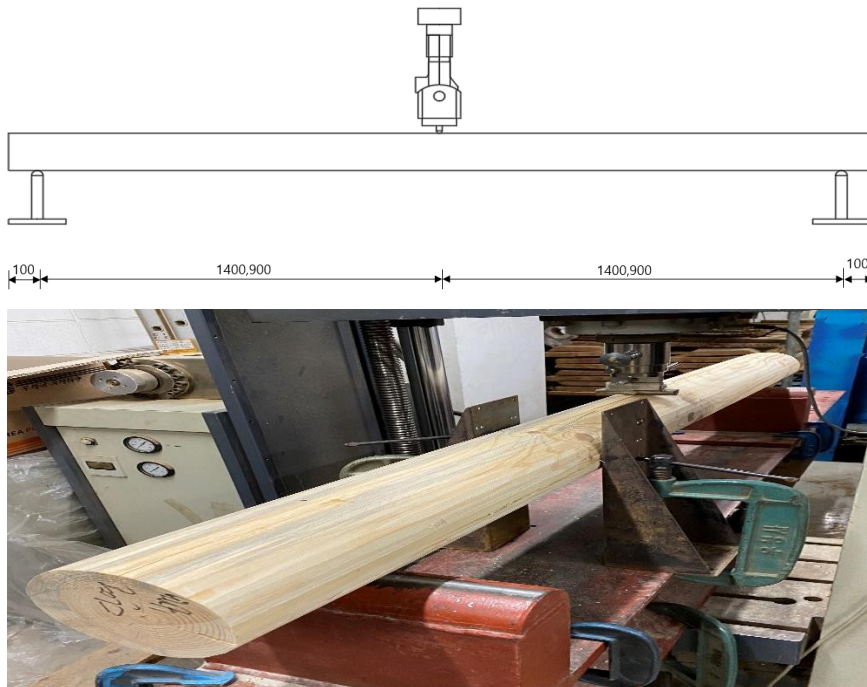


Figure 5-7 Test set-up (Yeon-mok)

5.1.4 Bu-yeon

1) Repair introduction

It was found that the length of the Bu-yeon of Lecture Hall of Sosu Confucian Academy provided by the foundation was shortened due to damage to the fixing nail part of the back root, and the cross section was reduced due to severe damage to the side part. If the repair method is considered based on this, it is difficult to apply the oblique scarf joint and the butt joint. Therefore, this

experiment tries to figure out the flexural and shearing performance of the designed Bu-yeon by applying a tusk tenon joint (Figure 5-8).

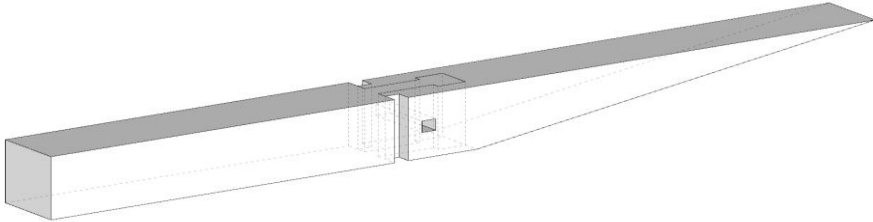


Figure 5-8 The tusk tenon joint (Bu-yeon)

2) Repair design

The sizes of the reference member and the repaired member of Bu-yeon were manufactured based on the experimental members provided by the foundation. The cross section (width \times height) of Bu-yeon was set to be 100mm \times 110mm, the length was 1200mm, the head to Bu-yeon Chak-go was set to 500mm, and the groove to the Bu-yeon Chak-go was set to 20mm \times 20mm. From Bu-yeon Chak-go to the root, 680 mm was set, among which, the section with a constant section was set to 100 mm, and the section with a decreasing section was set to 580 mm. The repaired member was made using tusk tenon joint. The total length of the tenon is 120mm, of which the length of the tenon neck is 80mm, the width of the tenon neck is 30mm, the length of the tenon head is 40mm, and the width of the tenon head is 50mm. A square wooden nail (20mm \times 20mm) was inserted because a gap occurred due to a manufacturing error when the head and the root of the repaired material were combined.

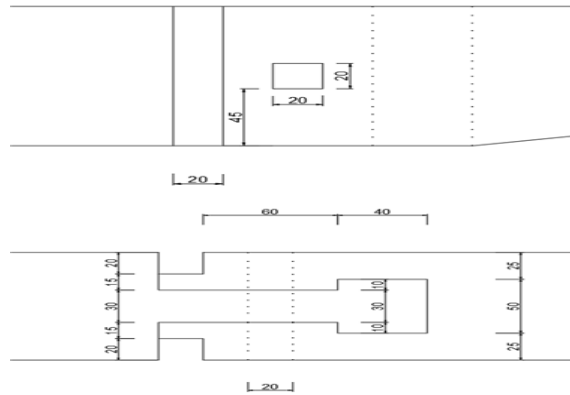


Figure 5-9 Detail of the repaired member (bu-yeon)

3) Experiment

The members of Bu-yeon had a length of 1200 mm and a reaction point of 510 mm at the head, which is the Bu-yeon Chak-go, and 190 mm at the root, referring to the shear force diagram in Chapter 3. Structural Analysis. The loading point was set at 540 mm from the root, which is the center of the resultant force of the tile load and the soil load. The loading was carried out using a 10-ton UTM machine, and the loading speed was 5 mm/min.

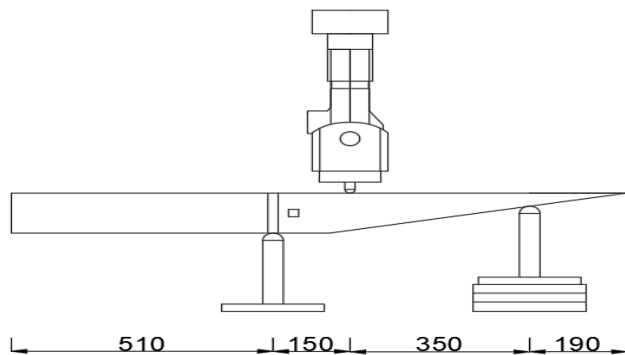




Figure 5-10 Test set-up (Bu-yeon)

5.1.5 Mok-gi-yeon

1) Repair introduction

Like Bu-yeon, the Mok-gi-yeon of Yangjindang House, which was provided by the foundation, was shortened in length due to damage to the fixing nail part at the root, and the cross section was reduced due to severe damage to the side. Based on this, when the repaired method is considered, it is difficult to apply the oblique scarf joint and the butt joint. Therefore, this experiment tries to figure out the bending and shearing performance of the designed Mok-gi-yeon by applying a tusk tenon joint.

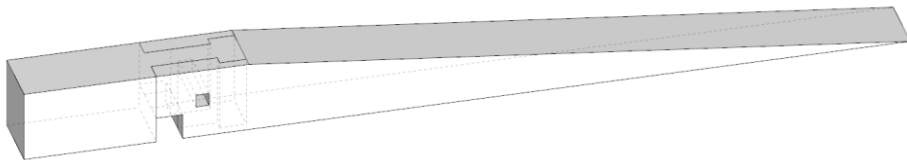


Figure 5-11 The tusk tenon joint (Mok-gi-yeon)

Chapter 5. Repair design and experiments

2) Repair design

The size of the reference member and the repaired member of Mokgi Yeon was manufactured based on the experimental members provided by the foundation. The cross section (width \times height) of Mok-gi-yeon was set to 100mm \times 110mm, the length was 1340mm, the head to the gable board was 200mm, and the gabled groove was set to 40mm \times 40mm. The length from the gable board to the root was 1100 mm. Among them, the section in which the cross section of the root part is constant was set to 100 mm, and the section in which the cross section was decreased was set to 1000 mm. The repaired member was made using tusk tenon joint. The total length of the tenon is 140mm, of which the length of the tenon neck is 100mm, the width of the tenon neck is 40mm, the length of the tenon head is 40mm, and the width of the tenon head is 70mm. A square wooden nail (20mm \times 20mm) was inserted because a gap occurred due to a manufacturing error when the head and the root of the repaired material were combined.

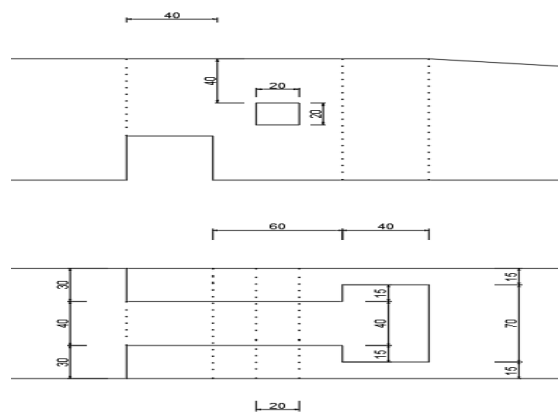


Figure 5-12 Detail of the repaired member (Mok-gi-yeon)

3) Experiment

The members of mok-gi-yeon are 1340 mm. With reference to the actual measurement drawings, the upper surface of Jang-yeon, which is the actual reaction point of Mok-gi-yeon, was assumed as the reaction point. The assumed reaction point is 240mm from the head, which is the gable board point, and 300mm and 700mm from the end of the root, which is the upper surface of Jang-yeon. Since the lifting of the root part occurs when the head part is loaded, the steel jig and the member were fixed with clamps. The loading point was set as the 100mm point of the head where the load of the gable ridge is concentrated. The loading was carried out using a 10-ton UTM machine, and the loading speed was 5 mm/min.

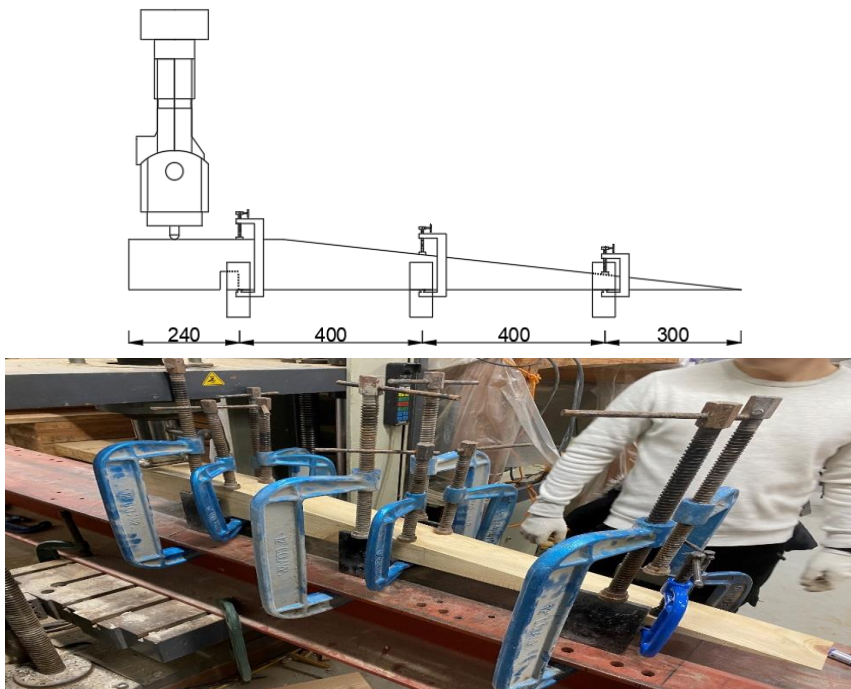


Figure 5-13 Test set-up (Mok-gi-yeon)

5.2 Experiment results and discussions

All measurement data were collected by a data logger through a LVDT (Linear Vertical Displacement Transducer). By converting the collected data, the relationship between load and stress and strain was analyzed. Since the yield load is not clear on the load-displacement graph, the intersection of the initial stiffness in the elastic region and the tangent in the plastic region was calculated as the yield load. The initial stiffness and stiffness in plastic region of the member were calculated with reference to ACI committee 363. The failure mode occurred as a flexural failure in the structural vulnerable part (Refer to Appendix. B.).

5.2.1 Load-displacement Curve

The load-displacement curve (Figure 5-14 - Figure 5-18) was analyzed for the results of the Flexure test. Analysis of the results will proceed in the order of yield load, ultimate load, stiffness, and stress.

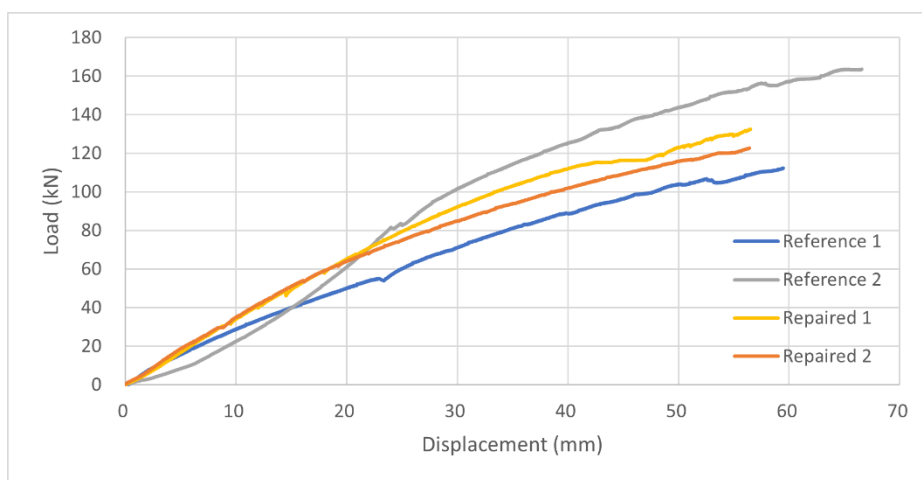


Figure 5-14 Load-Displacement curve (Chu-nyu)

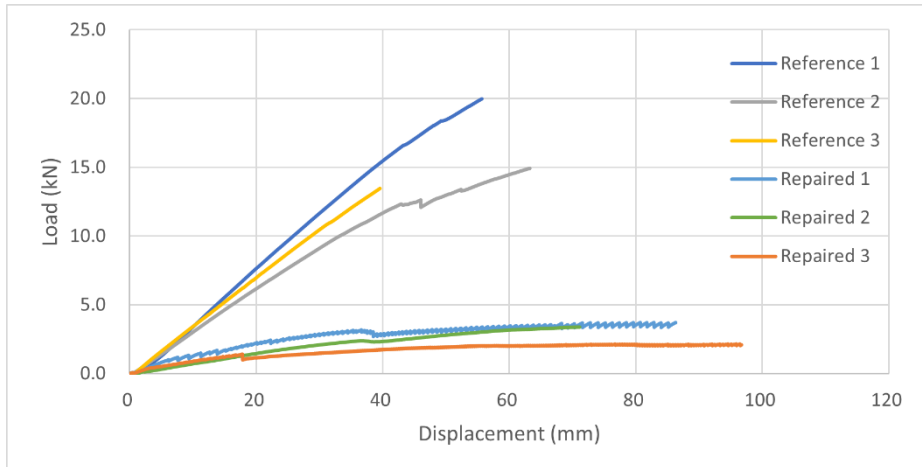


Figure 5-15 Load-Displacement curve (Jang-yeon)

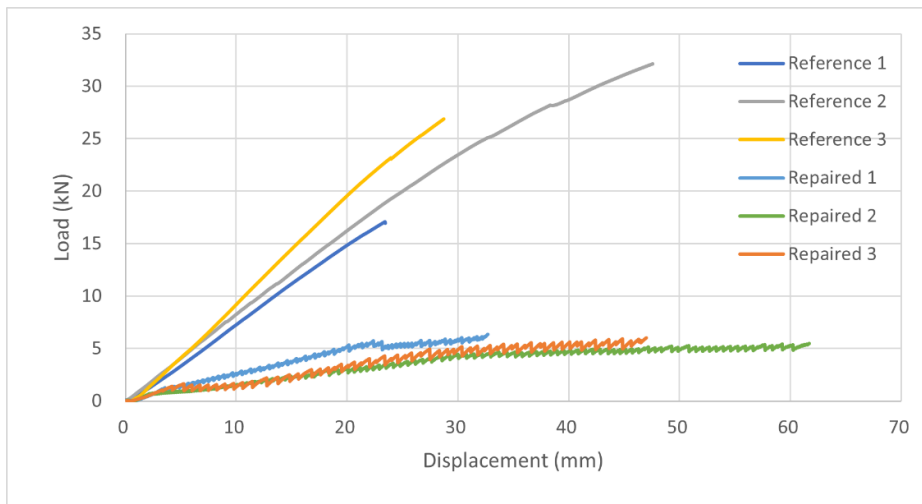


Figure 5-16 Load-Displacement curve (Dan-yeon)

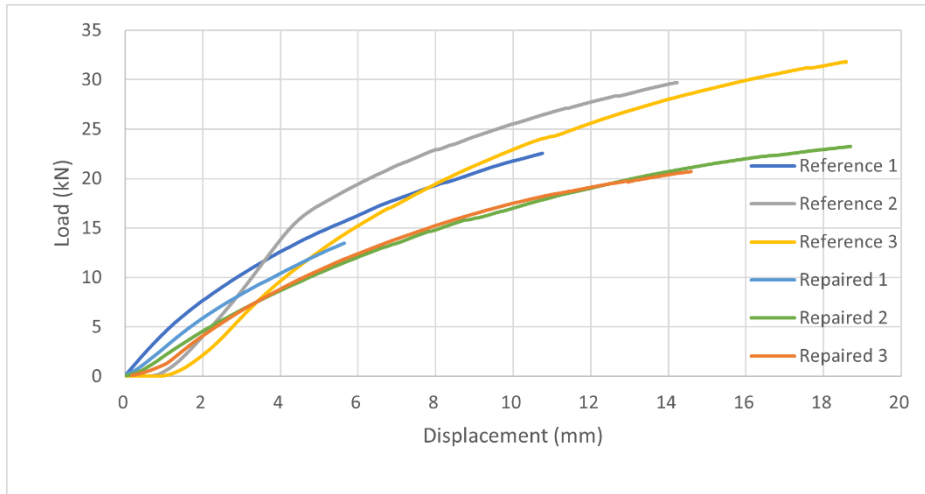


Figure 5-17 Load-Displacement curve (Bu-yeon)

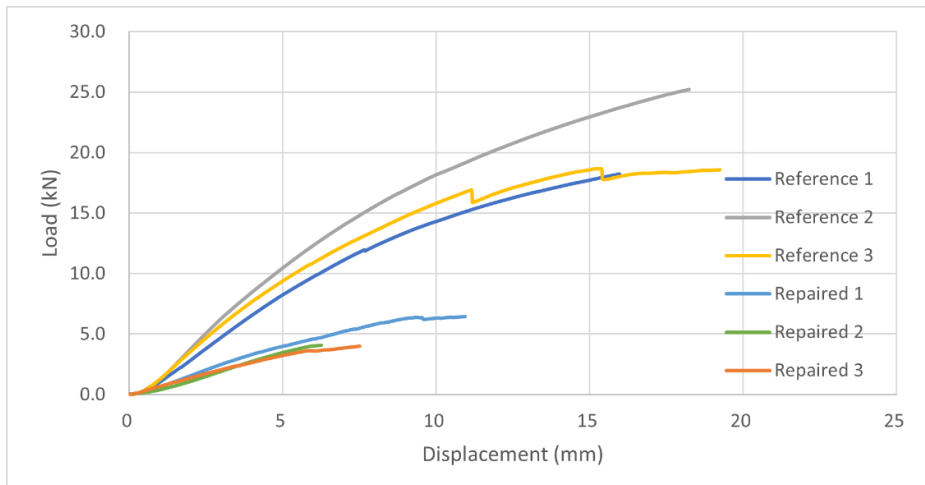


Figure 5-18 Load-Displacement curve (Mok-gi-yeon)

5.2.2 Strength

The reference member of Chu-nyu has a yield load of 90.44kN and an ultimate load of 138.02kN. The yield load of the repaired member was 80.96kN, which decreased by 10.5%. The ultimate load was 127.65kN, which decreased by 7.5% (Table 5-4).

Table 5-4 Load and displacement (Chu-nyu)

Member	Yield				Ultimate			
	P_y (kN)		δ_y (mm)		P_u (kN)		δ_u (mm)	
Reference 1	79.98	90.44	34.35	32.12	112.38	138.02	59.46	63.01
Reference 2	100.89		29.89		163.66		66.56	
Repaired 1	88.92	80.96	28.67	26.34	132.52	127.65	56.51	56.46
Repaired 2	73.00		24.01		122.77		56.41	

The reference member of Jang-yeon has a yield load of 10.19kN and an ultimate load of 16.12kN. The yield load of the repaired member was 1.84kN, which decreased by 81.9%. The ultimate load was 3.09kN, which decreased by 80.9% (Table 5-5).

Table 5-5 Load and displacement (Jang-yeon)

Member	Yield				Ultimate			
	P_y (kN)		δ_y (mm)		P_u (kN)		δ_u (mm)	
Reference 1	11.7	10.19	30.11	29.70	19.98	16.12	55.67	52.83
Reference 2	10.39		34.71		14.93		63.25	
Reference 3	8.48		24.28		13.46		39.56	
Repaired 1	2.5	1.84	24.2	23.41	3.71	3.09	86.3	84.72
Repaired 2	1.95		27.51		3.39		71.13	
Repaired 3	1.07		18.51		2.16		96.72	

Chapter 5. Repair design and experiments

The reference member of Dan-yeon has a yield load of 16.31kN and an ultimate load of 25.36kN. The yield load of the repaired member was 4.93kN, which decreased by 69.8%. The ultimate load was 5.95kN, which decreased by 76.5% (Table 5-6).

Table 5-6 Load and displacement (Dan-yeon)

Member	Yield				Ultimate			
	P_y (kN)		δ_y (mm)		P_u (kN)		δ_u (mm)	
Reference 1	9.82	16.31	13.26	19.56	17.08	25.36	23.45	33.25
Reference 2	21.98		27.81		32.13		47.58	
Reference 3	17.13		17.6		26.88		28.73	
Repaired 1	4.77	4.93	19.31	30.93	6.35	5.95	32.7	47.13
Repaired 2	4.54		34.94		5.48		61.7	
Repaired 3	5.47		38.53		6.02		47	

The reference member of Bu-yeon has a yield load of 13.67kN and an ultimate load of 28.03kN. The yield load of the repaired member was 10.81kN, which decreased by 20.9%. The ultimate load was 19.14kN, which decreased by 31.7% (Table 5-7).

Table 5-7 Load and displacement (Bu-yeon)

Member	Yield				Ultimate			
	P_y (kN)		δ_y (mm)		P_u (kN)		δ_u (mm)	
Reference 1	13.36	13.67	4.38	4.63	22.55	28.03	10.75	14.52
Reference 2	13.53		3.95		29.70		14.22	
Reference 3	14.12		5.55		31.84		18.58	
Repaired 1	7.04	10.81	2.45	5.07	13.47	19.14	5.64	12.97
Repaired 2	14.1		7.43		23.25		18.69	
Repaired 3	11.29		5.32		20.71		14.58	

The reference member of mok-gi-yeon has a yield load of 12.18kN and an ultimate load of 20.72kN. The yield load of the repaired member was 3.02kN, which decreased by 75.2%. The ultimate load was 4.85kN, which decreased by 76.6% (Table 5-8).

Table 5-8 Load and displacement (Mok-gi-yeon)

Member	Yield				Ultimate			
	P_y (kN)	12.18	δ_y (mm)	6.77	P_u (kN)	20.72	δ_u (mm)	17.82
Reference 1	10.74		6.72		18.24		15.98	
Reference 2	14.18	7.1	25.23	18.24				
Reference 3	11.62	6.5	18.69	19.25				
Repaired 1	3.87	4.8	6.45	10.94				
Repaired 2	2.4	3.57	4.09	6.26				
Repaired 3	2.78	4.21	4.00	7.51				

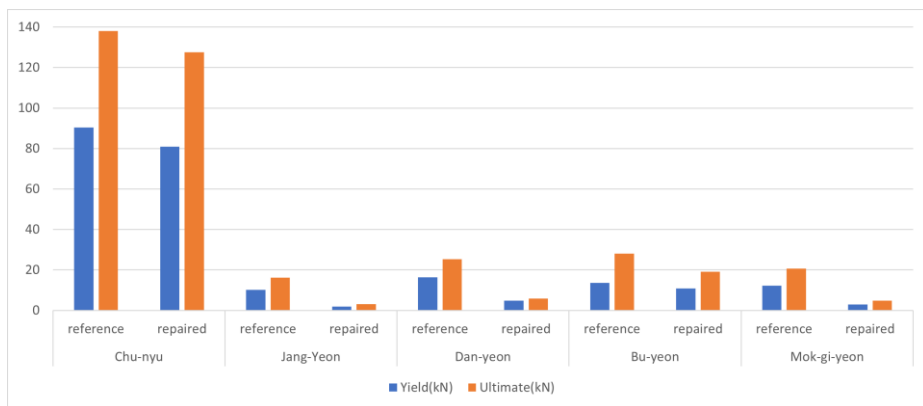


Figure 5-19 Comparing the yield and the ultimate load

As a result of comprehensive testing of roof members, it was found that the flexural strength of the repaired members by the traditional carpentry method

decreased compared to the reference members. The closest to the flexural strength of the reference member was the Chu-nyu, followed by Bu-yeon, Dan-yeon, Mok-gi-yeon, and Jang-yeon. In particular, Jang-yeon showed a decrease rate of over 80%.

5.2.3 Stiffness

The stiffness can be calculated from the slope of the load-displacement curve. The stiffness can be divided into the initial stiffness in the elastic region (K_E) and the stiffness in the plastic region (K_P). Each stiffness was calculated based on the following equation of ACI Committee 363.

$$K_E = \frac{P_y}{\delta_y}, \quad K_P = \frac{P_u - P_y}{\delta_u - \delta_y}$$

In accordance with the above equation, the initial stiffness in the elastic region and the stiffness in the plastic region were calculated based on the load and displacement at the yield load and ultimate load.

In the reference member of the Chu-nyu, the initial stiffness is 2.85 and the stiffness in the plastic region is 1.50. The repaired member had an initial stiffness of 3.07, which increased by 8%, and a plastic stiffness of 1.56, which increased by 3%.

Table 5-9 Stiffness (Chu-nyu)

Member	Initial stiffness		Stiffness in the plastic region	
	Stiffness (kN/mm)	Repaired /Reference (%)	Stiffness (kN/mm)	Repaired /Reference (%)
Reference 1	2.33	1.00	1.29	1.00
Reference 2	3.38	1.00	1.71	1.00
Repaired 1	3.10	1.08	1.57	1.04
Repaired 2	3.04	1.07	1.54	1.02

In the reference member of the Jang-yeon, the initial stiffness is 0.35 and the stiffness in the plastic region is 0.27. The repaired member had an initial stiffness of 0.08, which decreased by 77.6%, and a plastic stiffness of 0.02, which decreased by 91.8%.

Table 5-10 Stiffness (Jang-yeon)

Member	Initial stiffness		Stiffness in the plastic region	
	Stiffness (kN/mm)	Repaired /Reference (%)	P_u (kN)	Stiffness (kN/mm)
Reference 1	0.39	1.0	0.32	1.0
Reference 2	0.30	1.0	0.16	1.0
Reference 3	0.35	1.0	0.33	1.0
Repaired 1	0.10	0.30	0.02	0.07
Repaired 2	0.07	0.21	0.03	0.12
Repaired 3	0.06	0.17	0.01	0.05

In the reference member of the Dan-yeon, the initial stiffness is 0.83 and the stiffness in the plastic region is 0.70. The repaired member had an initial stiffness of 0.17, which decreased by 79.2%, and a plastic stiffness of 0.07,

Chapter 5. Repair design and experiments

which decreased by 89.6%.

Table 5-11 Stiffness (Dan-yeon)

Member	Initial stiffness		Stiffness in the plastic region	
	Stiffness (kN/mm)	Repaired /Reference (%)	P_u (kN)	Stiffness (kN/mm)
Reference 1	0.74	1.0	0.71	1.0
Reference 2	0.79	1.0	0.51	1.0
Reference 3	0.97	1.0	0.88	1.0
Repaired 1	0.25	0.30	0.12	0.17
Repaired 2	0.13	0.16	0.04	0.05
Repaired 3	0.14	0.17	0.06	0.09

In the reference member of the Bu-yeon, the initial stiffness is 3.01 and the stiffness in the plastic region is 1.46. The repaired member had an initial stiffness of 2.30, which decreased by 23.6%, and a plastic stiffness of 1.28, which decreased by 12.1%.

Table 5-12 Stiffness (Bu-yeon)

Member	Initial stiffness		Stiffness in the plastic region	
	Stiffness (kN/mm)	Repaired /Reference (%)	P_u (kN)	Stiffness (kN/mm)
Reference 1	3.05	1.0	1.44	1.0
Reference 2	3.43	1.0	1.57	1.0
Reference 3	2.54	1.0	1.36	1.0
Repaired 1	2.87	0.96	2.02	1.38
Repaired 2	1.90	0.63	0.81	0.56
Repaired 3	2.12	0.71	1.02	0.70

In the reference member of the Mok-gi-yeon, the initial stiffness is 1.79 and the stiffness in the plastic region is 0.79. The repaired member had an initial stiffness of 0.71, which decreased by 60.3%, and a plastic stiffness of 0.47, which decreased by 39.8%.

Table 5-13 Stiffness (Mok-gi-yeon)

Member	Initial stiffness		Stiffness in the plastic region	
	Stiffness (kN/mm)	Repaired /Reference (%)	P_u (kN)	Stiffness (kN/mm)
Reference 1	1.60	1.0	0.81	1.0
Reference 2	2.00	1.0	0.99	1.0
Reference 3	1.79	1.0	0.55	1.0
Repaired 1	0.81	0.45	0.42	0.53
Repaired 2	0.67	0.37	0.63	0.80
Repaired 3	0.66	0.37	0.37	0.47

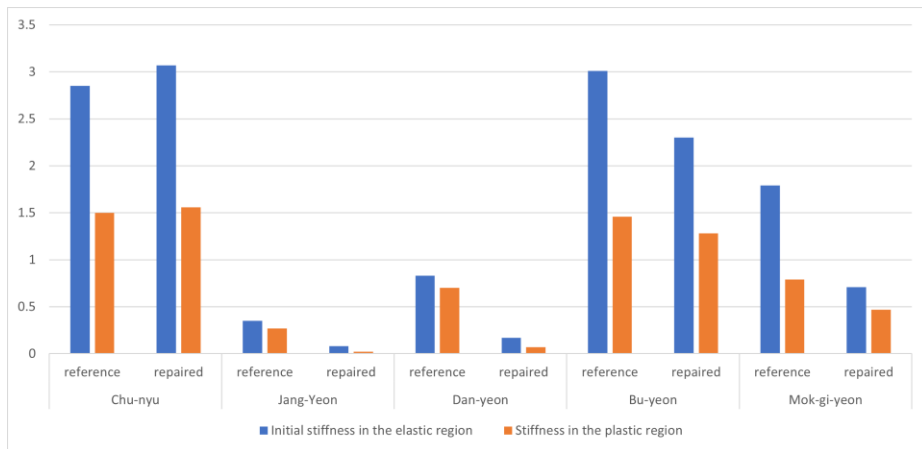


Figure 5-20 Comparing the stiffness

5.2.4 Ductility

Ductility (μ_u) applies the concept that a structure will fail when it can no longer support the load. Through the displacement (δ_y) at yield and the displacement (δ_u) at fracture of the member, the ductility coefficient was calculated by the following equation.

$$\mu_u = \delta_u / \delta_y$$

In the reference member of the Chu-nyu, the ductility is 1.98. The repaired member had a ductility of 2.16, which increased by 9%.

Table 5-14 Ductility (Chu-nyu)

Member	Ductility coefficient		Ductility ratio	
	μ_u	Average	Repaired /Reference (%)	Average
Reference 1	1.73	1.98	1.00	1.00
Reference 2	2.23		1.00	
Repaired 1	1.97	2.16	1.00	1.09
Repaired 2	2.35		1.19	

In the reference member of the Jang-yeon, the ductility is 1.77. The repaired member had a ductility of 3.79, which increased by 115%.

Table 5-15 Ductility (Jang-Yeon)

Member	Ductility coefficient		Ductility ratio	
	μ_u	Average	Repaired /Reference (%)	Average
Reference 1	1.85	1.77	1.00	1.00
Reference 2	1.82		1.00	
Reference 3	1.63		1.00	
Repaired 1	3.57	3.79	2.02	2.15
Repaired 2	2.59		1.46	
Repaired 3	5.23		2.96	

In the reference member of the Dan-yeon, the ductility is 1.70. The repaired member had a ductility of 1.56, which decreased by 8%.

Table 5-16 Ductility (Dan-yeon)

Member	Ductility coefficient		Ductility ratio	
	μ_u	Average	Repaired /Reference (%)	Average
Reference 1	1.77	1.70	1.00	1.00
Reference 2	1.71		1.00	
Reference 3	1.63		1.00	
Repaired 1	1.69	1.56	0.99	0.92
Repaired 2	1.77		1.04	
Repaired 3	1.22		0.72	

In the reference member of the Bu-yeon, the ductility is 3.13. The repaired member had a ductility of 2.52, which decreased by 20%.

Chapter 5. Repair design and experiments

Table 5-17 Ductility (Bu-yeon)

Member	Ductility coefficient		Ductility ratio	
	μ_u	Average	Repaired /Reference (%)	Average
Reference 1	2.45	3.13	1.00	1.00
Reference 2	3.60		1.00	
Reference 3	3.35		1.00	
Repaired 1	2.30	2.52	0.73	0.80
Repaired 2	2.52		0.80	
Repaired 3	2.74		0.87	

In the reference member of the Mok-gi-yeon, the ductility is 2.64. The repaired member had a ductility of 1.94, which decreased by 26%.

Table 5-18 Ductility (Mok-gi-yeon)

Member	Ductility coefficient		Ductility ratio	
	μ_u	Average	Repaired /Reference (%)	Average
Reference 1	2.38	2.64	1.00	1.00
Reference 2	2.57		1.00	
Reference 3	2.96		1.00	
Repaired 1	2.28	1.94	0.86	0.74
Repaired 2	1.75		0.67	
Repaired 3	1.78		0.68	

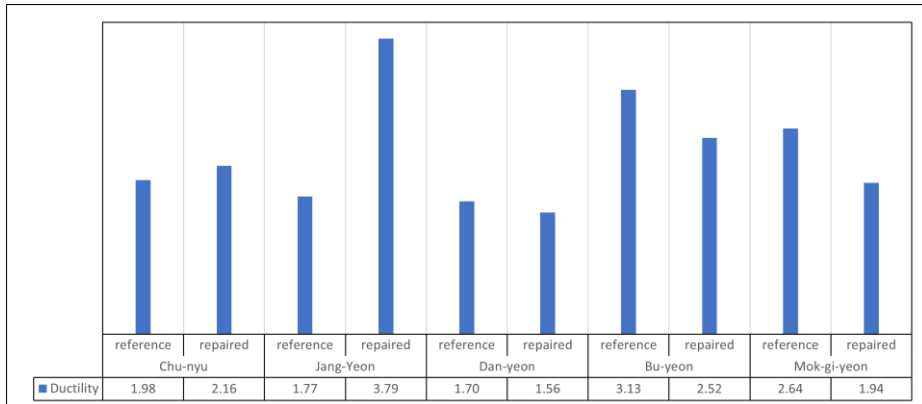


Figure 5-21 Comparing the ductility

5.2.5 Experimental value comparing theoretical value of reference

The experimental value and the theoretical value of reference member were compared using the ultimate load obtained from the experiment of each member. For the experimental value, Midas Gen, a general-purpose structural analysis program, was used. The bending moment was calculated by designing the member in the same form as the experimental conditions and inputting the ultimate load. The bending stress was calculated using the bending moment ($M/Z=\sigma$). The theoretical value was applied to the bending stress value of the wood used.

As a result of comparing the experimental and theoretical values in the reference member, the ratio was 34-48% for Chu-nyu, 61-91% for Jang-yeon, 50-94% for Dan-yeon, 25-36% for Bu-yeon, and 67~93% for Mok-gi-yeon. Experimental values tended to be lower than theoretical values (Table 5-19).

Chapter 5. Repair design and experiments

The reason for the low experimental value is the reduction of the bending stress of the member according to the lumbering process of the wood used as the member, the material characteristics of each, the strength difference between the sapwood and the heartwood, and the position of the knot of the wood.

Table 5-19 Experimental value comparing theoretical value of reference member

Member (R=reference)	Experimental flexural stress	Theoretical flexural stress	Experimental/ Theoretical(%)
Chu-nyu, R 1	16.1 MPa	46.6 MPa	34.5
Chu-nyu, R 2	22.5 MPa	46.6 MPa	48.3
Jang-yeon, R 1	42.2 MPa	46.6 MPa	90.6
Jang-yeon, R 2	31.5 MPa	46.6 MPa	67.7
Jang-yeon, R 3	28.4 MPa	46.6 MPa	61.0
Dan-yeon, R 1	23.2 MPa	46.6 MPa	49.8
Dan-yeon, R 2	43.6 MPa	46.6 MPa	93.6
Dan-yeon, R 3	36.6 MPa	46.6 MPa	78.3
Bu-yeon, R 1	11.7 MPa	46.6 MPa	25.2
Bu-yeon, R 2	15.5 MPa	46.6 MPa	33.2
Bu-yeon, R 3	16.6 MPa	46.6 MPa	35.6
Mok-gi-yeon, R 1	31.3 MPa	46.6 MPa	67.1
Mok-gi-yeon, R 2	43.3 MPa	46.6 MPa	92.8
Mok-gi-yeon, R 3	32.0 MPa	46.6 MPa	68.8

5.3 Section analysis model

5.3.1 Chu-nyu

In this experiment, the member to be repaired and the backing member are made of the same wood, and the modulus of elasticity is the same. Therefore, there is no significant difference in the stress distribution of the cross section between the reference member and the repaired member. However, if it is made of other wood, the modulus of elasticity obtained based on the test method standards of KS F 2150 can be used. By substituting the elastic modulus of each member into the transformed-section method, which converts the cross section of a composite beam into an equivalent section of a virtual beam composed of only one material, the stress distribution of the cross section can be theoretically inferred.

5.3.2 Yeon-mok

1) The modified butt joint

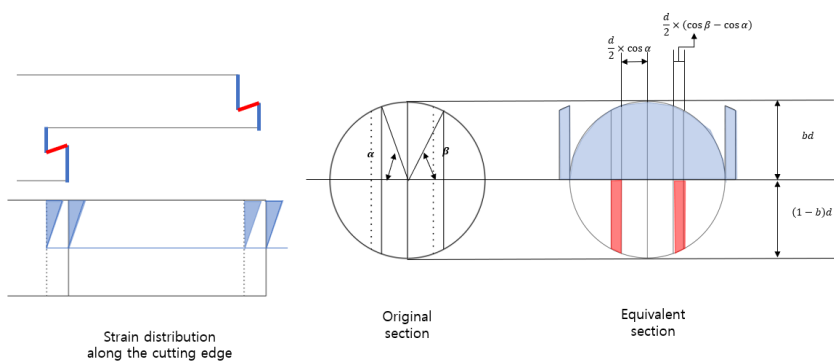


Figure 5-22 Equivalent section of modified butt joint

Chapter 5. Repair design and experiments

For modified butt joint, an equivalent cross-sectional model at the joint can be applied as shown in the Figure 5-22. Through the equivalent sectional model of the modified butt joint, the flexural strength ratio and flexural stiffness ratio between members can be estimated. If the curvature(k) at the joint and the height of the neutral axis are constant within the section, the position of the neutral axis and the moment of inertia of the equivalent section can be calculated through the force equilibrium condition. Additionally, it is assumed that the red area projected into the cross section of Yeon-mok resists bending. α is the angle between the neutral axis and the tenon neck, and β is the angle between the neutral axis and the tenon head. b is the ratio of the neutral axis, and d is the diameter of the Yeon-mok. In the Figure 5-22, the neutral axis passes through the center of the circle, but it is located closer to the top surface than the center of the circle. The equation derived by the force equilibrium condition is as follows.

Neutral axis:

$$\begin{aligned} \sum F_x &= 0; \\ \frac{k}{2} \int_{-\sqrt{(1-b)bd}}^{\sqrt{(1-b)bd}} \left(\sqrt{\left(\frac{d}{2}\right)^2 - x^2} - \left(\frac{1}{2} - b\right)d \right)^2 dx \\ &+ k \int_{\frac{1}{2}d \cos \alpha}^{\frac{1}{2}d \cos \beta} \left(\sqrt{\left(\frac{d}{2}\right)^2 - x^2} - \left(\frac{1}{2} - b\right)d \right)^2 dx \\ &= k \int_{\frac{1}{2}d \cos \alpha}^{\frac{1}{2}d \cos \beta} \left(\sqrt{\left(\frac{d}{2}\right)^2 - x^2} + \left(\frac{1}{2} - b\right)d \right)^2 dx \end{aligned}$$

Moment ratio:

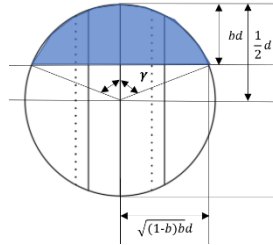


Figure 5-23 Location of angle γ

Additional variables were assigned to calculate the moment of inertia of the equivalent section. γ shows the angle between the neutral axis and the center of the circle (Figure 5-23). If the moment ratio is calculated using the variable, it is as follows.

$$M = E \times I_{eff} \times \phi$$

$$I_{eff} = \frac{d^4}{64} \times (3\alpha - 3\beta - 3 \sin \alpha \cos \alpha + 3 \sin \beta \cos \beta - 2 \sin^3 \alpha \cos \alpha + 2 \sin^3 \beta \cos \beta) \\ + \frac{d^4}{192} (3\gamma - 3 \sin \gamma \cos \gamma - 2 \sin^3 \gamma \cos \gamma) \\ + \left[\left(\frac{1}{2} - b \right) d \right]^2 \times \frac{d^2}{4} \times (\alpha - \beta - \gamma - \sin \alpha \cos \alpha + \sin \beta \cos \beta + \sin \gamma \cos \gamma)$$

$$I_g = \frac{\pi d^4}{64}$$

$$I_{eff}/I_g = \frac{2}{3\pi} \times (3\alpha - 3\beta - 3 \sin \alpha \cos \alpha + 3 \sin \beta \cos \beta - 2 \sin^3 \alpha \cos \alpha + 2 \sin^3 \beta \cos \beta) \\ + \frac{1}{3\pi} (3\gamma - 3 \sin \gamma \cos \gamma - 2 \sin^3 \gamma \cos \gamma) \\ + \left[\left(\frac{1}{2} - b \right) d \right]^2 \times \frac{16}{\pi d^2} \times (\alpha - \beta - \gamma - \sin \alpha \cos \alpha + \sin \beta \cos \beta + \sin \gamma \cos \gamma)$$

Chapter 5. Repair design and experiments

Substituting the size of the tested member into the above equation, β is 0.2996, and I_{eff}/I_g is 24.9%. The experimental results showed that the flexural strength ratio was 19.2%(Jang-yeon), 23.5%(Dan-yeon) and the initial stiffness was 22.9%(Jang-yeon), 20.5%(Dan-yeon). The flexural stiffness similar to the theoretical value, and the flexural strength showed a rather low value. It is judged that the initial stiffness was predicted relatively accurately because the equivalent sectional model assumed an initial state with little deformation.

Table 5-20 Flexural strength and initial stiffness (Jang-yeon)

Member	Flexural strength (kN · mm)	Initial stiffness (kN/mm)
Reference	11.29(100%)	0.35(100%)
Repaired	2.17(19.2%)	0.08(22.9%)

Table 5-21 Flexural strength and initial stiffness (Dan-yeon)

Member	Flexural strength (kN · mm)	Initial stiffness (kN/mm)
Reference	5.71(100%)	0.83(100%)
Repaired	1.34(23.5%)	0.17(20.5%)

5.3.3 Bu-yeon, Mok-gi-yeon

1) Tusk tenon joint

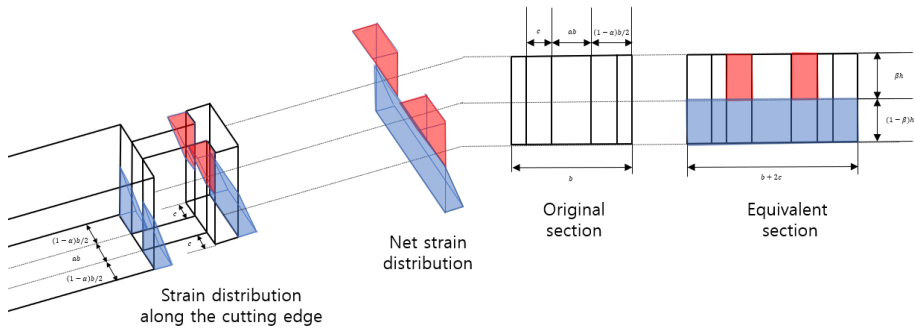


Figure 5-24 Equivalent section of tusk tenon joint

For tusk tenon joint, an equivalent cross-sectional model at the joint can be applied as shown in the Figure 5-24. If the curvature(k) at the joint and the height of the neutral axis are constant within the section, the position of the neutral axis and the moment of inertia of the equivalent section can be calculated through the force equilibrium condition. α is the ratio of the length of the tenon neck to the width of the member, β is the ratio of the height of the neutral axis, b is the width of the member, c is the width of the tenon head minus the width of the tenon neck, and h is the height of the member.

2) Bu-yeon

For the Bu-yeon to which the tusk tenon joint is applied, the Bu-yeon Chak-go groove should be considered in the equivalent cross-sectional model. The

Chapter 5. Repair design and experiments

width of the Bu-yeon Chak-go groove was defined as d . The equation derived by the force equilibrium condition is as follows.

Neutral axis:

$$\sum F_x = 0;$$

$$\beta h \times 2c \times k \times \beta h \times \frac{1}{2} = (b + 2c - 2d) \times (1 - \beta)h \times k \times (1 - \beta)h \times \frac{1}{2}$$

$$\therefore \beta = \frac{1}{1 + \sqrt{\frac{2c}{b + 2c - 2d}}}$$

Moment ratio:

$$M = E \times \left[\frac{1}{3} \times (2c \times \beta^3) + \frac{1}{3} \times (b + 2c - 2d) \times (1 - \beta)^3 \right] h^3 \times \phi$$

$$= E \times \frac{4}{b} \times [(2c \times \beta^3) + (b + 2c - 2d) \times (1 - \beta)^3] \times I_g \times \phi$$

$$= E \times I_{eff} \times \phi$$

$$\therefore I_{eff}/I_g = \frac{4}{b} \times [(2c \times \beta^3) + (b + 2c - 2d) \times (1 - \beta)^3]$$

Substituting the size of the tested member into the above equation, β is 0.667, and I_{eff}/I_g is 59.2%. The experimental results showed that the flexural strength ratio was 72% and the initial stiffness ratio was 76%, which is relatively higher than the theoretical values. A square wooden nail was inserted to prevent the slipping of the Bu-yeon, and it is judged that it had a relatively high bending resistance.

Table 5-22 Flexural strength and initial stiffness (Bu-yeon)

Member	Flexural strength (kN · mm)	Initial stiffness (kN/mm)
Reference	3.03(100%)	3.01(100%)
Repaired	2.01(72%)	2.30(76%)

3) Mok-gi-yeon

For the Mok-gi-yeon to which the tusk tenon joint is applied, the gable groove should be considered in the equivalent cross-sectional model. The height of the gable groove was defined as e . The equation derived by the force equilibrium condition is as follows.

Neutral axis:

$$\begin{aligned} \sum F_x &= 0; \\ \beta h \times 2c \times k \times \beta h \times \frac{1}{2} \\ &= (ab + 2c) \times (1 - \beta)h \times k \times (1 - \beta)h \times \frac{1}{2} \\ &\quad + (1 - \alpha)b \times [(1 - \beta)h - e] \times k \times [(1 - \beta)h - e] \times \frac{1}{2} \end{aligned}$$

Moment ratio:

$$\begin{aligned} M = E \times \left\{ \left[\frac{1}{3} \times (2c \times \beta^3) + \frac{1}{3} \times (ab + 2c) \times (1 - \beta)^3 \right] h^3 \right. \\ \left. + \frac{1}{3} \times (1 - \alpha)b \times [(1 - \beta)h - e]^3 \right\} \times \phi \end{aligned}$$

Chapter 5. Repair design and experiments

$$\begin{aligned}
 &= E \times \frac{4}{b} \times \left\{ [(2c \times \beta^3) + (\alpha b + 2c) \times (1 - \beta)^3] + \frac{1}{h^3} (1 - \alpha) b \times [(1 - \beta)h - e]^3 \right\} \times I_g \\
 &\quad \times \emptyset \\
 &= E \times I_{eff} \times \emptyset \\
 \therefore I_{eff}/I_g &= \frac{4}{b} \times \left\{ [(2c \times \beta^3) + (\alpha b + 2c) \times (1 - \beta)^3] + \frac{1}{h^3} (1 - \alpha) b \times [(1 - \beta)h - e]^3 \right\}
 \end{aligned}$$

Substituting the size of the tested member into the above equation, β is 0.627, and I_{eff}/I_g is 44.1%. The experimental results showed that the flexural strength ratio was 23% and the initial stiffness ratio was 40%. The flexural stiffness similar to the theoretical value, and the flexural strength showed a rather low value. It is judged that the initial stiffness was predicted relatively accurately because the equivalent sectional model assumed an initial state with little deformation.

Table 5-23 Flexural strength and initial stiffness (Mok-gi-yeon)

Member	Flexural strength (kN · mm)	Initial stiffness (kN/mm)
Reference	2.9(100%)	1.79(100%)
Repaired	0.68(23%)	0.71(40%)

Chapter 6. Conclusion

In this study, repair and reinforcement studies were conducted to reuse damaged members of Jeongyodang Hall in Dosanseowon Confucian School, Lecture Hall of Sosu Confucian Academy, Yangjindang House, Namhansanseong Suengyeoljeon Hall. In this study, structural analysis was conducted to identify structural vulnerable part. Decay part was identified by applying non-destructive diagnostic technology. Based on this, repair design and structural experiments were conducted, and a cross-sectional analysis model was created and reviewed using the results. Through the above process, the following conclusions could be obtained.

- 1) Through structural analysis, the vulnerable part of Chu-nyu, Yeon-mok, Bu-yeon, and Mok-gi-yeon were identified. Each the vulnerable part is Cheoma Do-ri, central point, Bu-yeon Chak-go, and the Gable board in order.
- 2) The vulnerable parts of decay are the upper part of Cheoma Do-ri (Chu-nyu), the edge of member (Yeon-mok), and the root part (Bu-yeon, Mok-gi-yeon).
- 3) The flexural strength ratio of the specimen decreased overall. The flexural strength ratio decreased by 7.5% for Chu-nyu, 80.9% for Jang-yeon, 76.5% for Dan-yeon, 31.7% for Bu-yeon and 76.6% for Mok-gi-yeon.
- 4) The bending stiffness ratio of the specimen decreased except for Chu-

Chapter 6. Conclusion

nyu. In Chu-nyu, the initial stiffness increased by 8% and the stiffness in the plastic region increased by 3%. Although the flexural stiffness and flexural strength were slightly different, the results were generally similar.

- 5) Ductility increased in Chu-nyu and Jang-yeon. Other absences decreased by 8% (Dan-yeon), 20% (Bu-yeon), and 26% (Mok-gi-yeon).
- 6) In the case of performing cross-sectional analysis through the equivalent sectional model, the results were more accurately matched to the initial stiffness assuming a state with little deformation.

In this study, only one variable was added to each member, and experiments and analysis were carried out. Since there are not many related studies, a basic study was conducted through the traditional carpentry method. It is considered that studies such as resin treatment on members, reinforcement of hardware, and various dimensions of joints are necessary.

Appendix. A. List of non-destructive test results

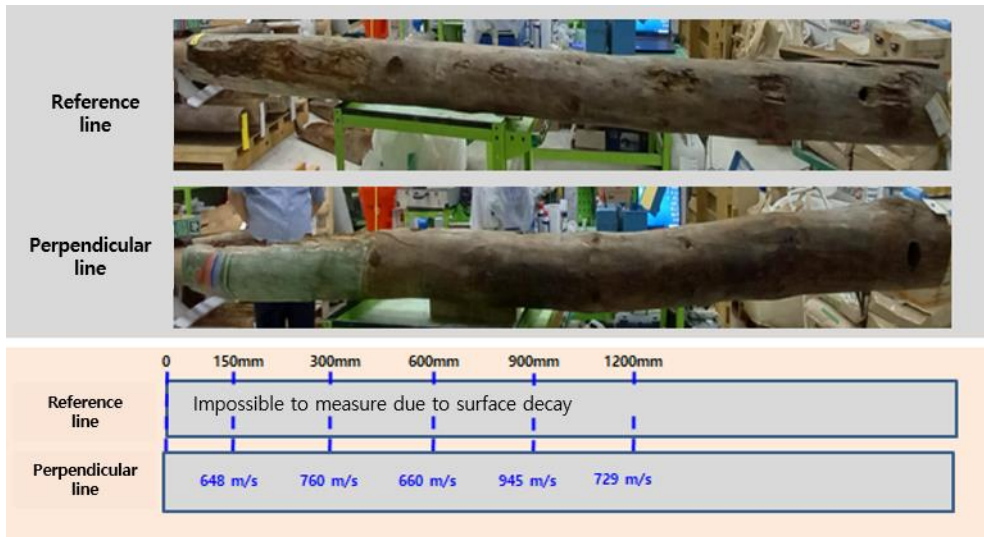


Figure Appendix.A. 1 Jang-yeon1 of Lecture Hall of Sosu

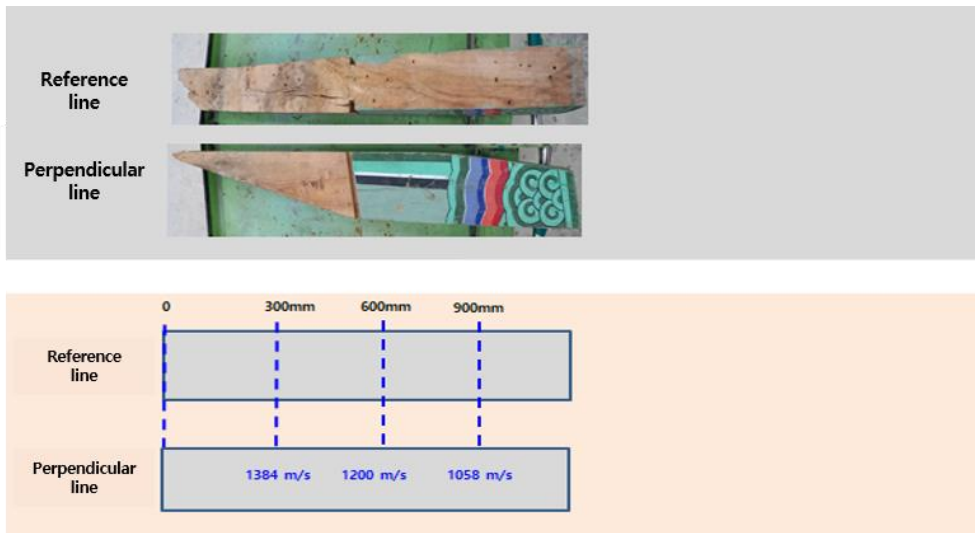


Figure Appendix.A. 2 Bu-yeon1 of Lecture Hall of Sosu

Appendix. A. List of non-destructive test results

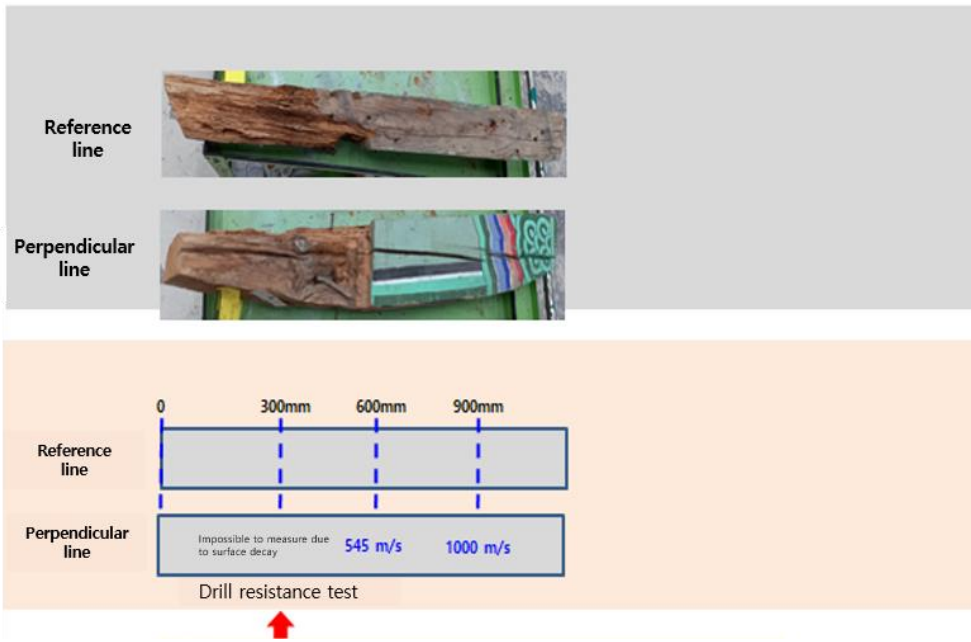


Figure Appendix.A. 3 Bu-yeon2 of Lecture Hall of Sosu

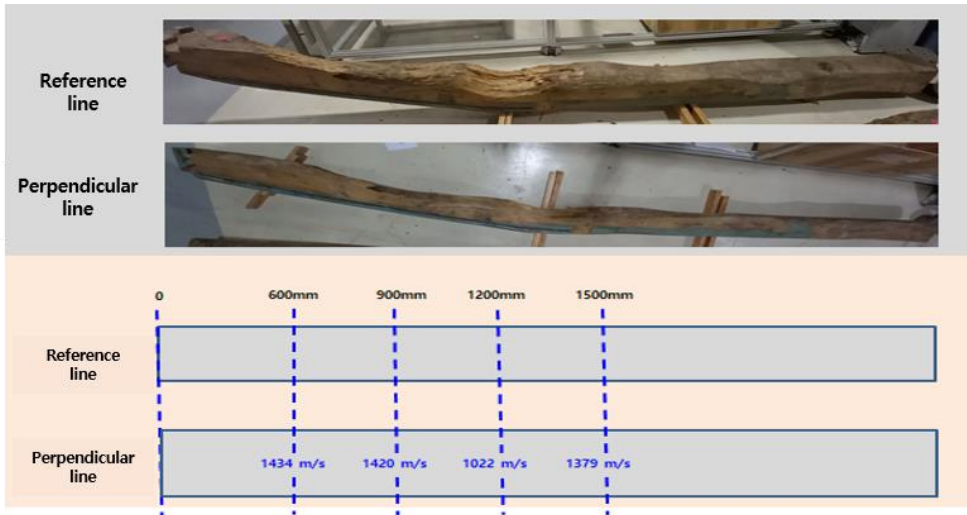


Figure Appendix.A. 4 Chu-nyul of Jeongyodang Hall

Appendix. A. List of non-destructive test results

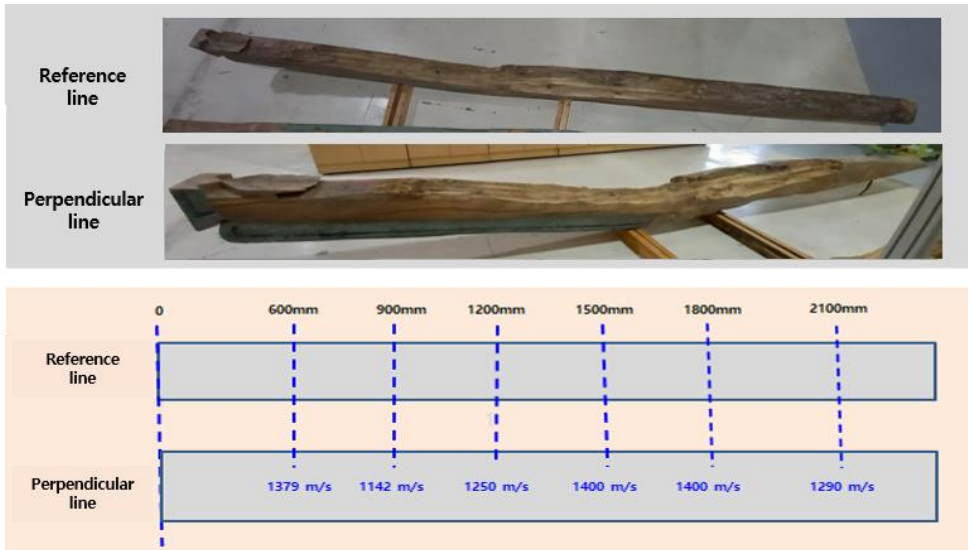


Figure Appendix.A. 5 Chu-nyu2 of Jeongyodang Hall

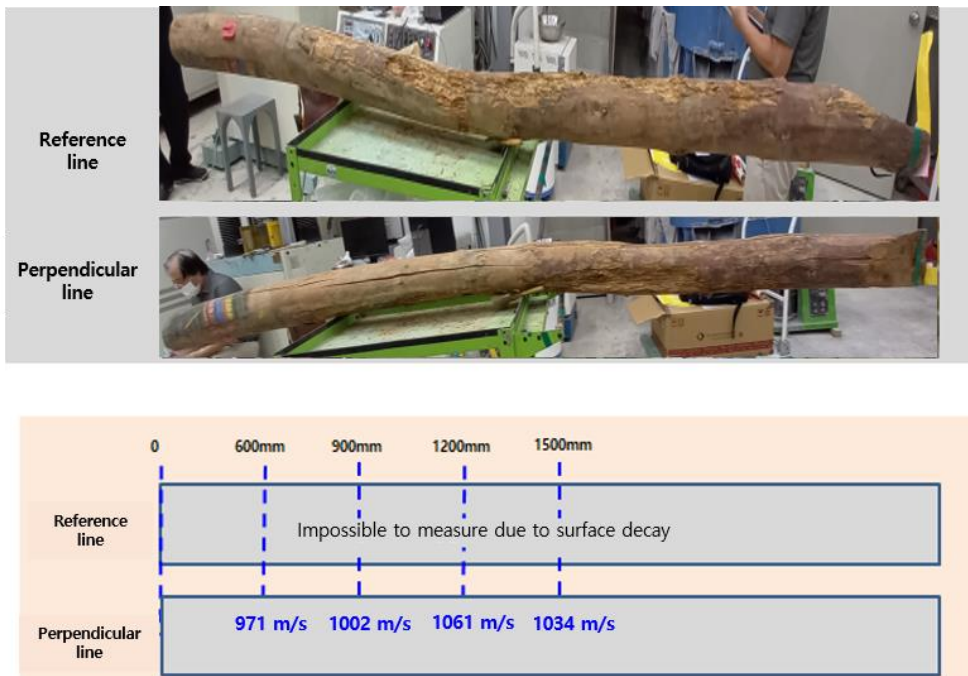


Figure Appendix.A. 6 Jang-yeon1 of Jeongyodang Hall

Appendix. A. List of non-destructive test results

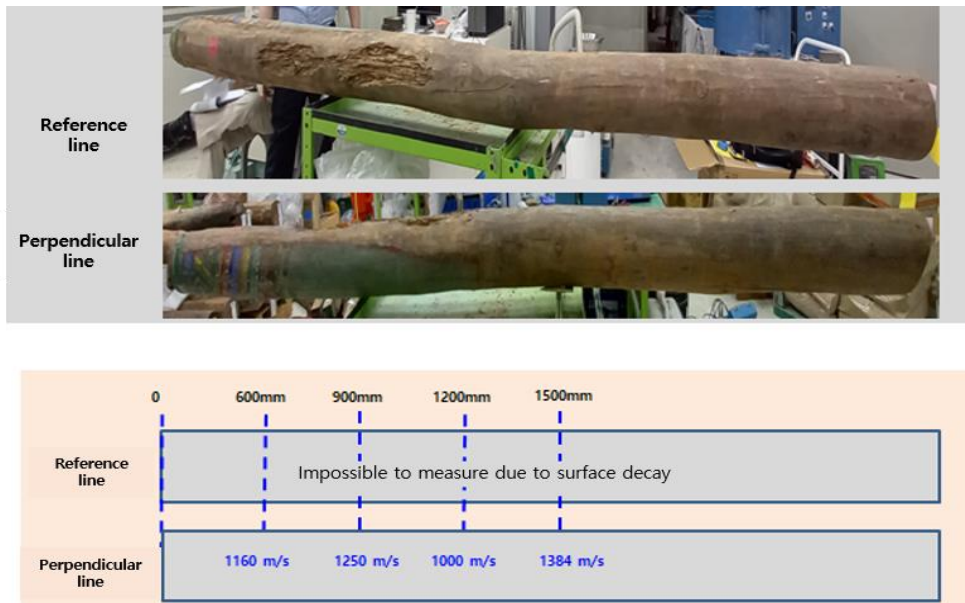


Figure Appendix.A. 7 Jang-yeon2 of Jeongyodang Hall

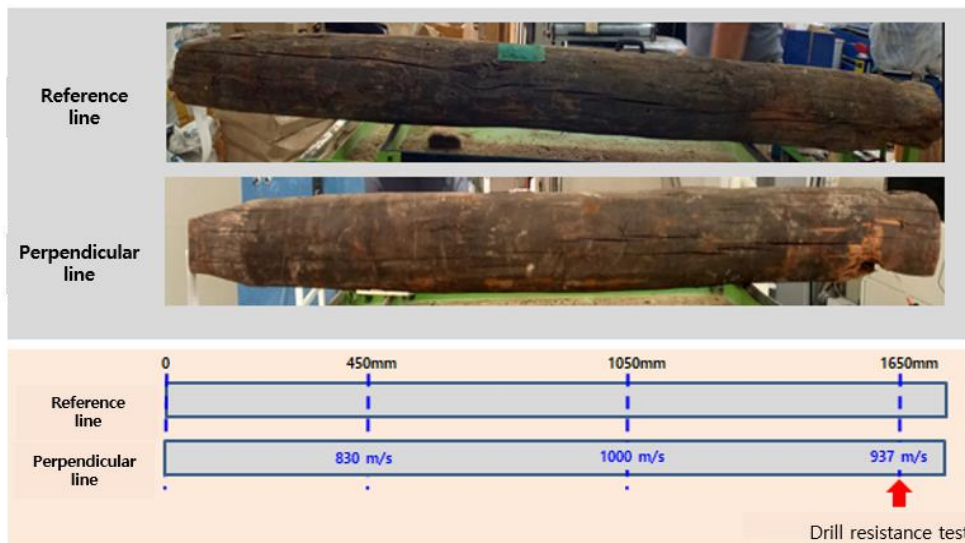


Figure Appendix.A. 8 Dan-yeon1 of Yangjindang House

Appendix. A. List of non-destructive test results

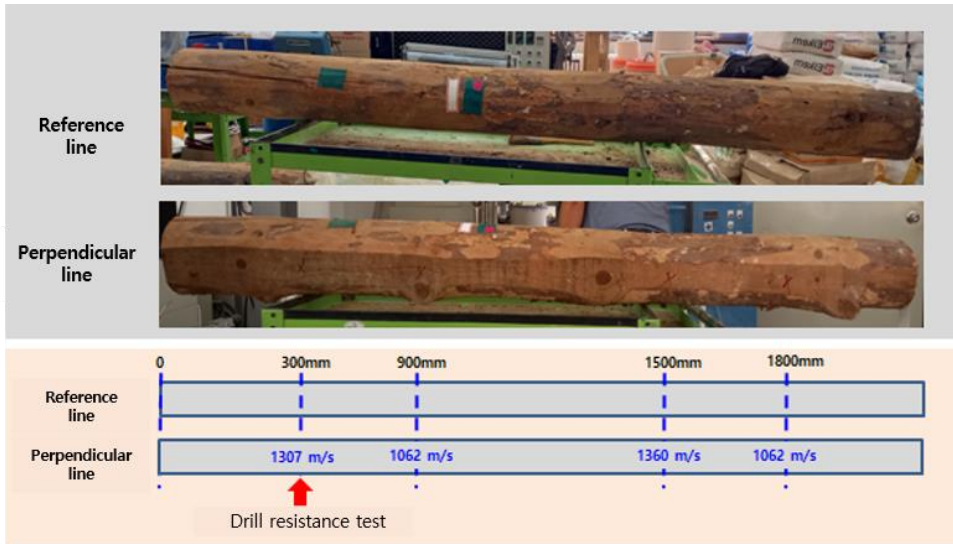


Figure Appendix.A. 9 Dan-yeon2 of Yangjindang House

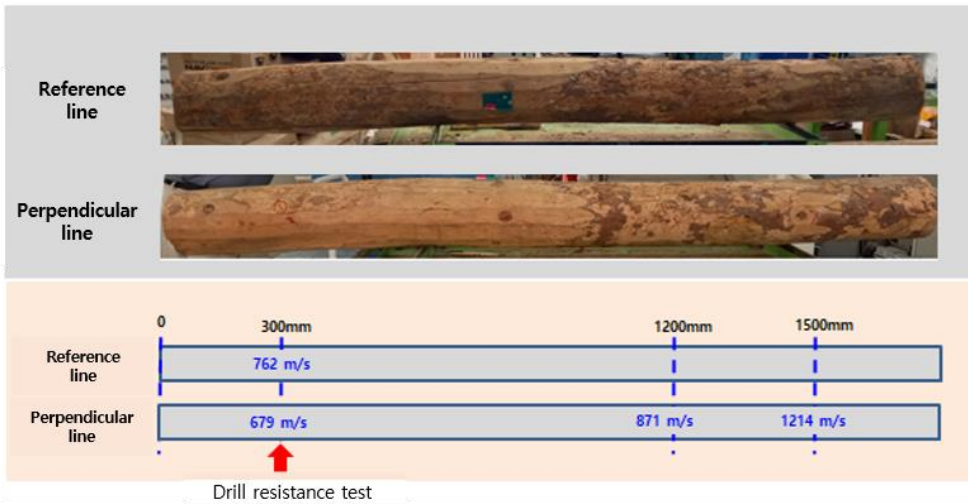


Figure Appendix.A. 10 Dan-yeon3 of Yangjindang House

Appendix. A. List of non-destructive test results

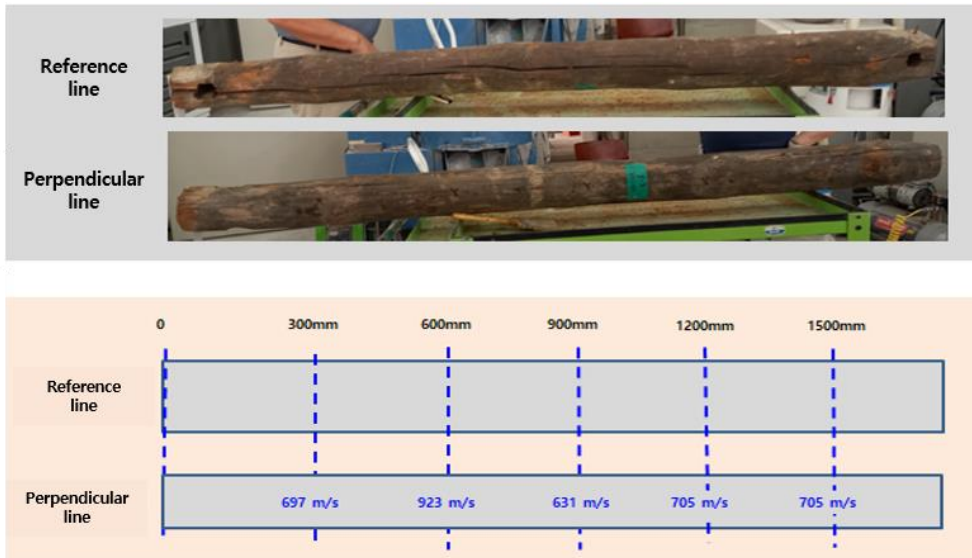


Figure Appendix.A. 11 Dan-yeon4 of Yangjindang House

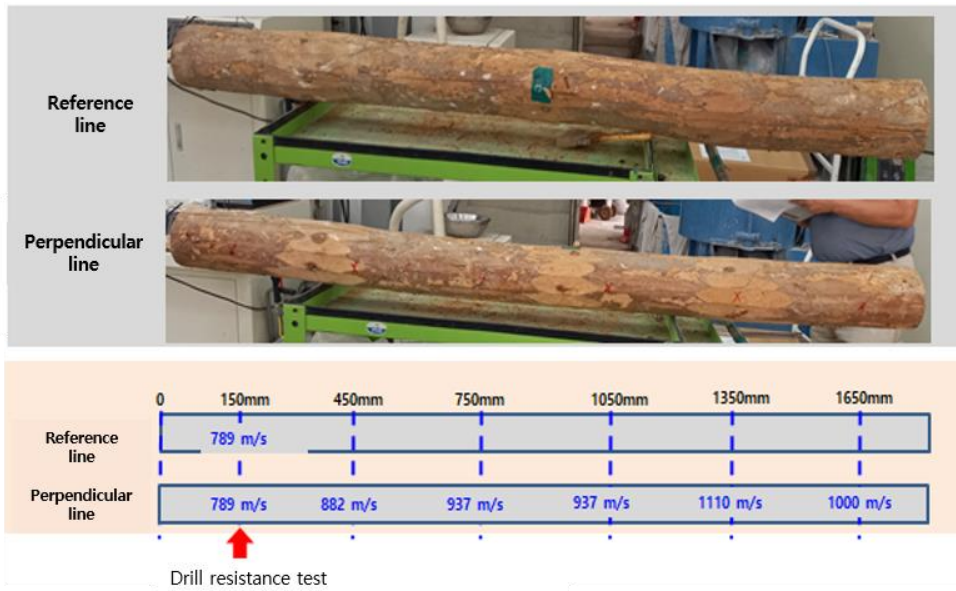


Figure Appendix.A. 12 Dan-yeon5 of Yangjindang House

Appendix. A. List of non-destructive test results

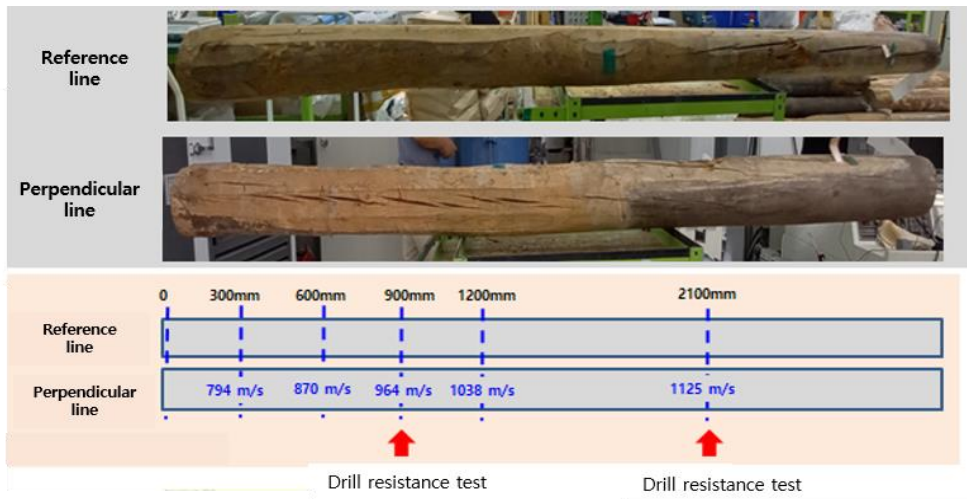


Figure Appendix.A. 13 Jang-yeon1 of Yangjindang House

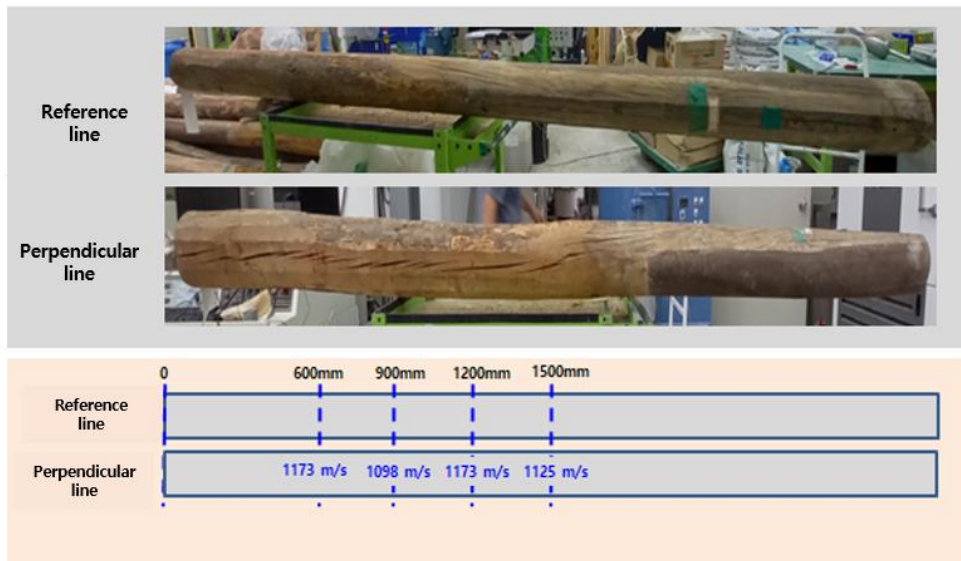


Figure Appendix.A. 14 Jang-yeon2 of Yangjindang House

Appendix. A. List of non-destructive test results

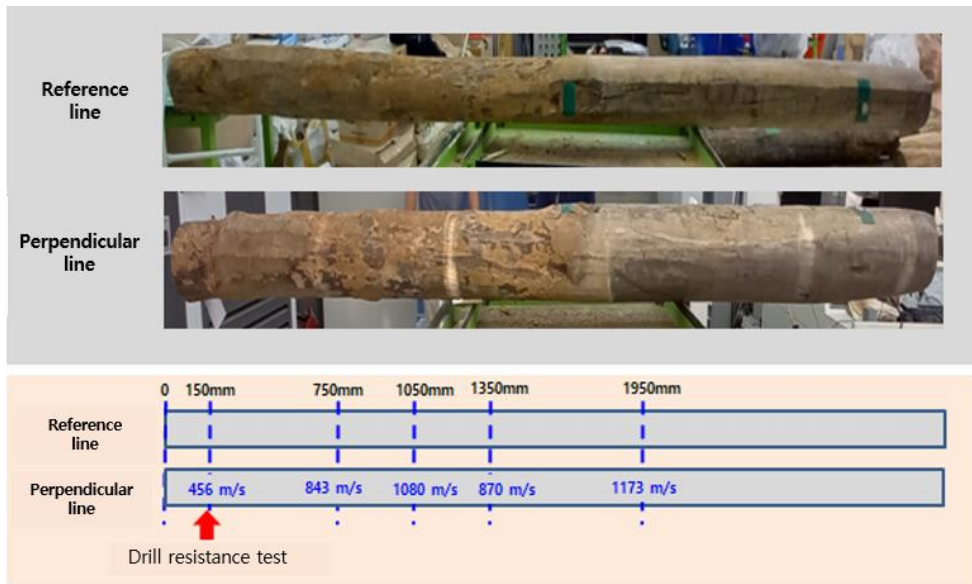


Figure Appendix.A. 15 Jang-yeon3 of Yangjindang House



Figure Appendix.A. 16 Jang-yeon4 of Yangjindang House

Appendix. A. List of non-destructive test results

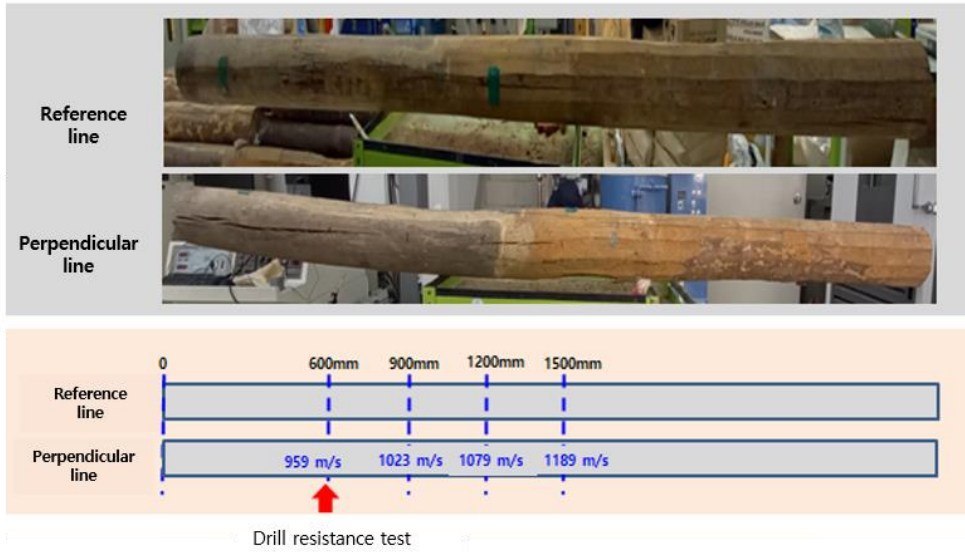


Figure Appendix.A. 17 Jang-yeon5 of Yangjindang House



Figure Appendix.A. 18 Jang-yeon6 of Yangjindang House

Appendix. A. List of non-destructive test results



Figure Appendix.A. 19 Jang-yeon7 of Yangjindang House



Figure Appendix.A. 20 Jang-yeon8 of Yangjindang House

Appendix. A. List of non-destructive test results

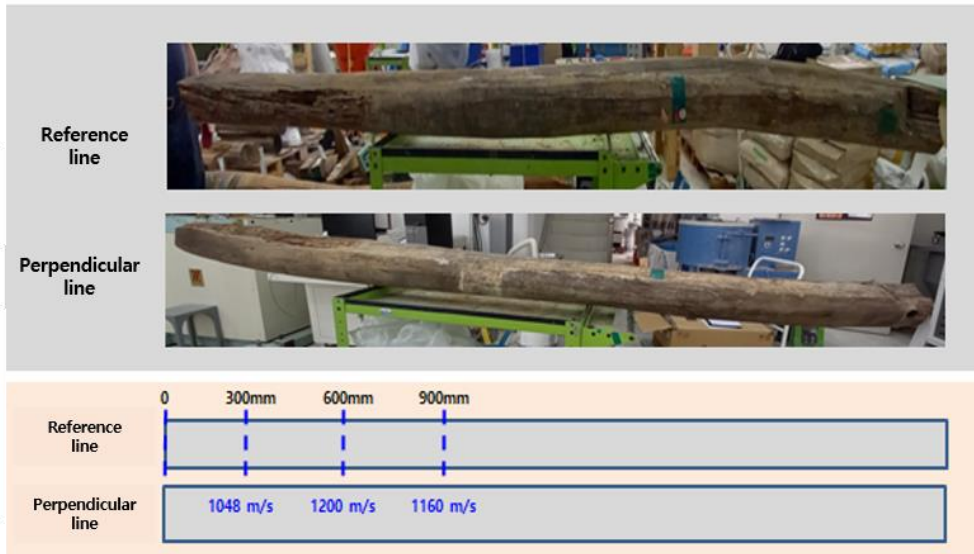


Figure Appendix.A. 21 Jang-yeon9 of Yangjindang House

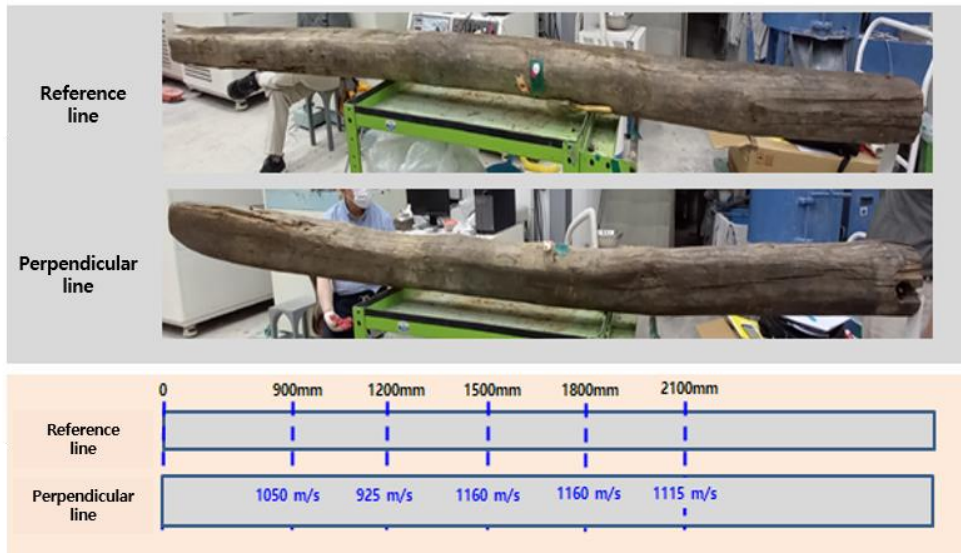


Figure Appendix.A. 22 Jang-yeon10 of Yangjindang House

Appendix. A. List of non-destructive test results

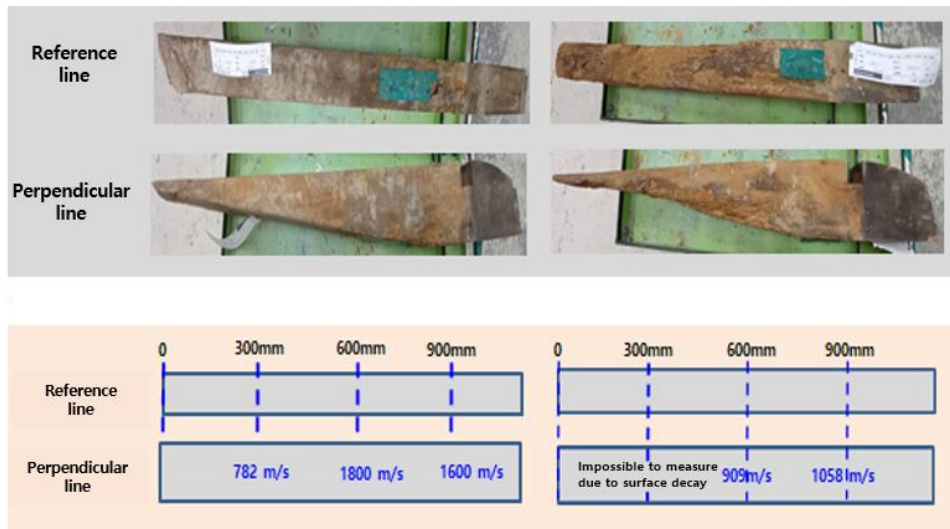


Figure Appendix.A. 23 Mok-gi-yeon1,2 of Yangjindang House

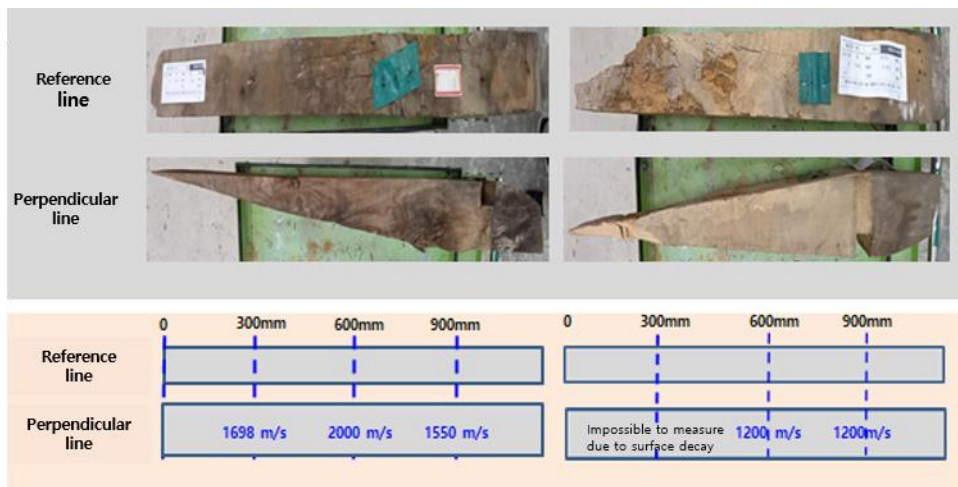


Figure Appendix.A. 24 Mok-gi-yeon3.4 of Yangjindang House

Appendix. A. List of non-destructive test results

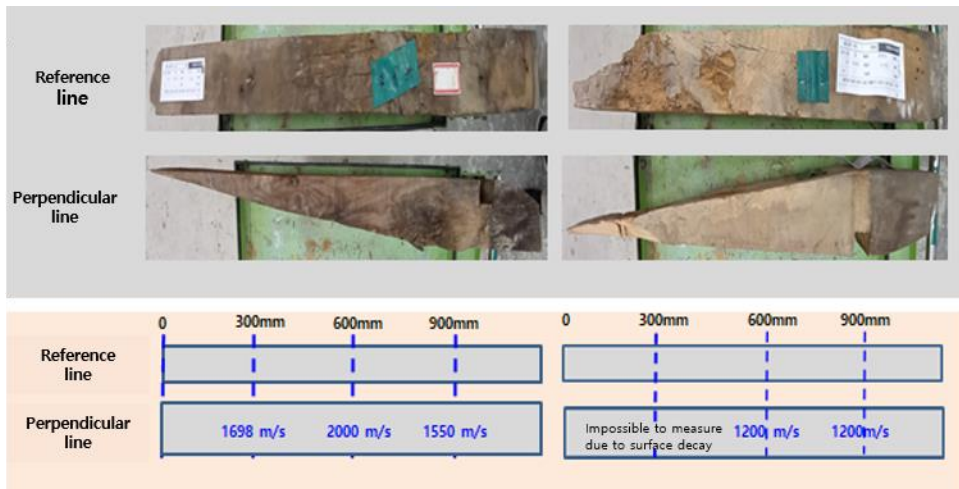


Figure Appendix.A. 25 Mok-gi-yeon3.4 of Yangjindang House

Appendix. B. Failure mode of flexural test



Figure Appendix.B. 1 Reference 1 of Chu-nyu



Figure Appendix.B. 2 Reference 2 of Chu-nyu



Figure Appendix.B. 3 Repaired 1 of Chu-nyu



Figure Appendix.B. 4 Repaired 2 of Chu-nyu

Appendix. B. Failure mode of flexural test



Figure Appendix.B. 5 Reference 1 (left), Reference 2 (right) of Jang-yeon



Figure Appendix.B. 6 Reference 3 (left), Repaired 1(right) of Jang-yeon

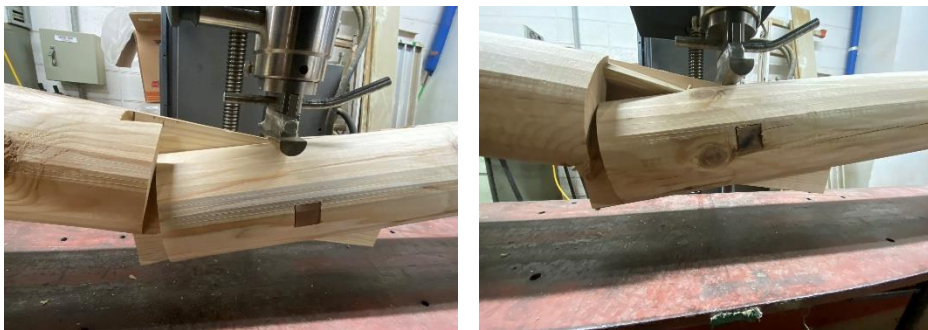


Figure Appendix.B. 7 Repaired 2 (left), Repaired 3 (right) of Jang-yeon

Appendix. B. Failure mode of flexural test



Figure Appendix.B. 8 Reference 1 (left), Reference 2 (right) of Dan-yeon



Figure Appendix.B. 9 Reference 3 (left), Repaired 1 (right) of Dan-yeon

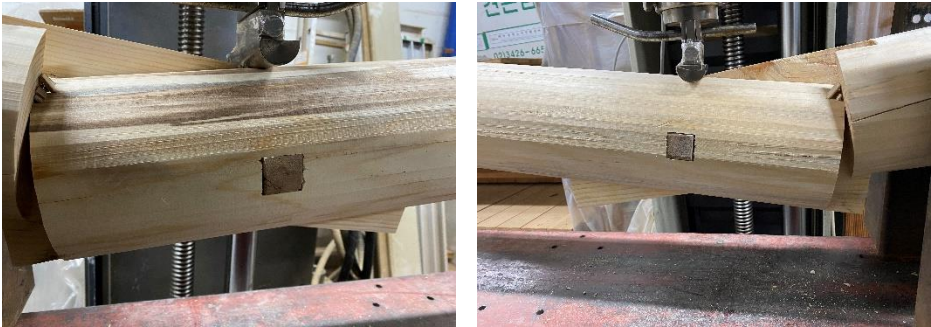


Figure Appendix.B. 10 Repaired 2 (left), Repaired 3 (right) of Dan-yeon

Appendix. B. Failure mode of flexural test



Figure Appendix.B. 11 Reference 1 of Bu-yeon

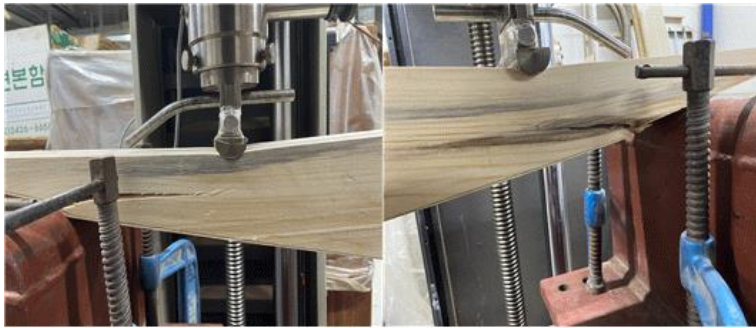


Figure Appendix.B. 12 Reference 2 of Bu-yeon



Figure Appendix.B. 13 Reference 3 of Bu-yeon

Appendix. B. Failure mode of flexural test



Figure Appendix.B. 14 Repaired 1 of Bu-yeon



Figure Appendix.B. 15 Repaired 2 of Bu-yeon



Figure Appendix.B. 16 Repaired 3 of Bu-yeon

Appendix. B. Failure mode of flexural test



Figure Appendix.B. 17 Reference 1 of Mok-gi-yeon



Figure Appendix.B. 18 Reference 2 of Mok-gi-yeon



Figure Appendix.B. 19 Reference 3 of Mok-gi-yeon

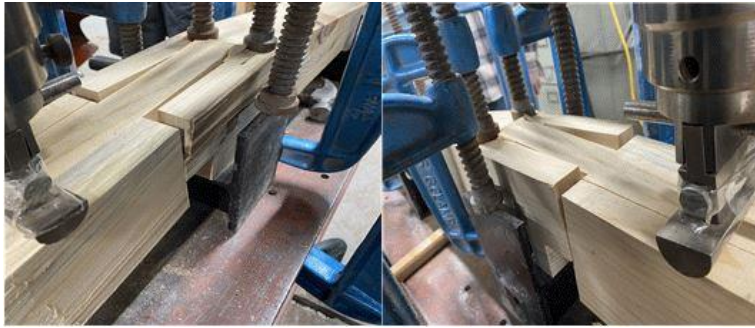


Figure Appendix.B. 20 Repaired 1 of Mok-gi-yeon



Figure Appendix.B. 21 Repaired 2 of Mok-gi-yeon



Figure Appendix.B. 22 Repaired 3 of Mok-gi-yeon

References

- [1] Steffen Franke, Bettina Franke, and Annette M. Harte, 2015, “Failure modes and reinforcement techniques for timber beams-state of the art”, *Construction and Building Materials*, Vol 97, pp. 2-13
- [2] Kang, H., 2016, “Concept of ‘original form’ in architectural heritage and its relationship with conservation-Focusing on the critical analysis on the past practices of timber building in Korea”, *Korean Journal of Cultural Heritage Studies*, Vol. 49(1), pp. 120-145.
- [3] Kim, Y. M., and Kim, J. H., 2011, “Structure-based Research Trends in Traditional Wood Structure and Proposal for Future Research Direction”, conference of architectural institute of korea - structural part, Vol. 31(2), pp. 3-4.
- [4] Jo, S. S., Kim, H. K., and Park, B. M., 2005, “Evaluation of Safety by Structural Analysis of Traditional Wooden Building, *Journal of Korea Institute for Structural Maintenance and Inspection*, Vol. 9(4), pp. 149-158.
- [5] Lee, J. J., Kim, K. C., and Bae, M. S, 2003, “Patterns of Resistographs for Evaluating Deteriorated Structural Wood Members”, *Journal of the Korean Wood Science and Technology*, Vol. 31(6), pp. 45-54.
- [6] Cho, C. H. ,Shin, Y. S., Cho, Y. H., No, S. R., and Kim, J. S., 2010, “A Study on the Structural Strengthening Characteristic of Traditional Wooden Architecture Hip Rafter in Hipped-and-gabled Roof, *Journal of The Architectural Institute of Korea Structure and Construction*, Vol.

- 26(3), pp. 8-10.
- [7] Kim, B. G., 1994, “A Study on the Korean traditional wooden architecture with multi-roof”, Graduate School of Seoul National University – Ph.D. dissertation
- [8] Kong, J. H., 2015, “Review of Visual Grading and Allowable Stress Determination Methodologies for Domestic Softwood”, Journal of Korean Wood Science and technology, Vol. 43(1), pp. 25-35.
- [9] Lee, S. J., 2008, “A Study on Structural Flexural Strengthening of Traditional Wooden Architecture”, Graduate School of Industry of Chosun University – M.S. thesis
- [10] Kim, S. C., Moon, Y. J., and Yang, I. S., 2009, “Flexural Performance of Strengthened Structural Laminated Timber Beams by Epoxy Bonded Fiber Sheets”, Journal of The Architectural Institute of Korea Structure and Construction, Vol. 25(12), pp. 39-46.
- [11] KS F 2201: 2021, “General requirements for testing of wood”
- [12] KS F 2206: 2020, “Method of compression test for wood”
- [13] KS F 2207: 2020, “Method of tension test for wood”
- [14] KS F 2208: 2020, “Method of bending test for wood”
- [15] KS F 2209: 2020, “Method of shear test for wood”
- [16] KS F 2150: 2020, “Method of static bending test for full sized structural lumber”

References

- [17] KDS 41 31 01: 2016, “wooden structure - General information”
- [18] KDS 41 31 02: 2016, “wooden structure - Material and allowable stress”
- [19] KDS 41 31 03: 2016, “wooden structure - Design requirements”
- [20] KDS 41 31 04: 2019, “wooden structure - Design of member”
- [21] KDS 41 31 05: 2016, “wooden structure - Design of joints”
- [22] KDS 41 31 06: 2016, “wooden structure - Traditional wooden structure”
- [23] ISO 6891:1983, “Timber structures-joints made with mechanical fasteners-general principles for the determination of strength and deformation characteristics”
- [24] ISO 8375:1985, “Solid timber in structural sizes-determination of some physical and mechanical properties”
- [25] ISO 8970:1985, “Timber structures-testing of joints made with mechanical fasteners-requirements for timber density”
- [26] ICOMOS, “The principle for the conservation of wooden built heritage”
- [27] ACI Committee 363, “High-Strength Concrete”

초 록

전통 목조 건축물의 지붕 부재 보수보강에 관한 연구

이 서 형

서울대학교 건축학과 대학원

전통 목조 건축물은 국가지정 문화재의 많은 비율을 차지하고 있다. 시간이 지남에 따라 목조 건축물은 다양한 요인의 손상을 받게 된다. 노후화된 전통 목조 건축물은 문화재보호법에 따라 꾸준히 보수공사가 이루어지고 있다. 수리 공사시 손상된 부재의 보수 기준이 명확치 않아 신재로 교체하는 것이 일반적이며 과도한 교체가 이루어지고 있다. 본 연구에서는 재사용 가능한 고부재의 무분별한 교체를 방지하기 위해 목조 문화재 지붕부재의 보수 보강에 관한 연구를 수행하였다.

현재 문화재와 관련된 연구는 목조 접합부의 강성에 대한 연구가 주를 이루며, 부재단위의 보수 보강 연구가 부족하다. 따라서 본 연구에서는 재단으로부터 도산서원 전교당, 소수서원 강학당, 상주 양진당, 승렬전 본전의 지붕부재를 제공받았으며, 이를 활용하여, 구조해석, 비파괴 검사, 보강설계, 단면해석을 진행하였다.

목조 문화재의 부재 단위 구조해석을 통하여 부재의 구조적 취약부를 검토하였고, 비파괴 검사를 하여 자연발생적 부후 취약부를 조사하였다. 보강 설계시, 사례조사를 통하여 각 부재의 하중조건에 맞는 전통적인 결구법을 적용하였다. 이음부의 성능을 검증하기 위해서 부재별 하중 조건에 부합하는 단순 가력 휨 실험을 수행하였다.

실험의 결과 값으로 휨강도, 휨강성, 연성을 산출하였다. 휨강도와 초기 휨강성은 비슷한 비율로 증감하는 경향을 보였다. 변형된 맞장부 이음과 방형 메뚜기 장부이음은 등가단면모형을 통하여 분석하였다. 등가단면모형은 초기 휨강성을 예측하는데 우수한 성능을 보였다.

추녀를 제외하면 크기가 작은 지붕부재(연목, 부연, 목기연 등)는 관련된 연구가 부족하다. 따라서 본 연구에서 제안된 모델은 기초적인 연구자료로써 활용할 수 있을 것으로 기대한다.

주요어: 목조 문화재, 지붕부재, 비파괴 검사, 보수보강, 단면해석모델

학 번 : 2019-23472